JOURNAL OF MATERIALS SCIENCE 24 (1989) 3421–3440

# Review
# Zirconia-toughened alumina (ZTA) ceramics

J. WANG, R. STEVENS
*School of Materials, University of Leeds, Leeds LS2, UK*

In the previous decade, a considerable amount of work has been done on the alumina–zirconia ceramic composite system with a particular emphasis on improving the mechanical properties utilizing the recognized toughening mechanisms. Zirconia-toughened aluminas (ZTA) can be regarded as a new generation of toughened ceramics; for example, a toughness of $> 12\,MPa\,m^{0.5}$ has been obtained, compared with $3\,MPa\,m^{0.5}$ for commercial alumina ceramics. The fracture strength of ZTA is also greatly in excess of that for alumina. The mechanical properties of ZTA are critically dependent on their microstructures, which can be designed in terms of specific applications and controlled by means of powder preparation and densification processes. This review also includes details of the possible future development of ZTA; these are expected to involve the development and measurement of the mechanical properties for high-temperature engineering applications.

## 1. Introduction

The introduction of zirconia into alumina as a sintering aid has long been practiced for densification of alumina engineering ceramics [1]. However, the concept of toughening alumina ceramics by dispersing zirconia particles in the matrix has only been recognized in the last ten years [2–6].

The introduction of a small amount (1000 to 2000 p.p.m.) of zirconia into alumina as a sintering aid allows the formation of a solid solution which promotes the densification processes by the introduction of lattice defects. In contrast, the microstructures of ZTA are characterized by the presence of the two distinct phases, which do not react with each other to form a solid solution [7]. The toughening of alumina by dispersing zirconia particles was first encouraged by the development of the partially stabilized zirconias (PSZ) [4]. The presence of zirconia grains in the alumina matrix as a discrete second phase enables the former to behave in an intrinsic manner, that is, to undergo the tetragonal → monoclinic transformation or to be retained as the metastable tetragonal form during cooling of the composites from the fabrication temperatures. It is the volume expansion and shear strain associated with the tetragonal → monoclinic transformation that results in various toughening mechanisms in these composites, including stress-induced transformation toughening, microcracking toughening, compressive surface stresses and crack deflection.

The ZTA composites considered in this review are, therefore, those that have a microstructure in which alumina and zirconia are present as two distinct phases, rather than as a solid solution.

## 2. Toughening mechanisms

The toughening mechanisms in ZTA are related to the volume expansion and shear strain associated with the tetragonal → monoclinic transformation. There are two well-accepted mechanisms which have been discussed in great detail in the literature [2, 5, 6, 8–11] stress-induced transformation toughening and microcrack toughening. Other possible mechanisms which enhance the mechanical properties have also been discussed, including the development of compressive surface stresses and crack deflection [8–12]. There follows a brief description which reviews these mechanisms individually.

### 2.1. Stress-induced transformation toughening

It is known that the metastable tetragonal zirconia inclusions which are dispersed in a ceramic matrix will transform to their thermodynamically stable monoclinic form on application of an external tensile stress around a crack tip [4, 5]. The phase transformation, which is accompanied by a volume expansion ($\sim 4\%$) and shear strain ($\sim 6\%$), will provide a compressive stress which acts to reduce and eventually stop the propagation of the crack, necessitating extra work for further crack propagation. Ruhle *et al.* [13] observed *in situ* the stress-induced transformation in ZTA using a high-resolution transmission electron microscope (HRTEM) which was fitted with a double-tilting straining stage. A great deal of intellectual energy has been expended in attempts to devise theories and develop mathematical frameworks to model the mechanism [14–21].

One of the well-established models is that developed by Evans *et al.* [11, 14–18, 22], who considered the transformation toughening as a crack-shielding process. They explained the shielding in terms of a process zone, Fig. 1a, which is a source of stress and displacement disturbance that tends to shield the

0022–2461/89 $03.00 + .12 

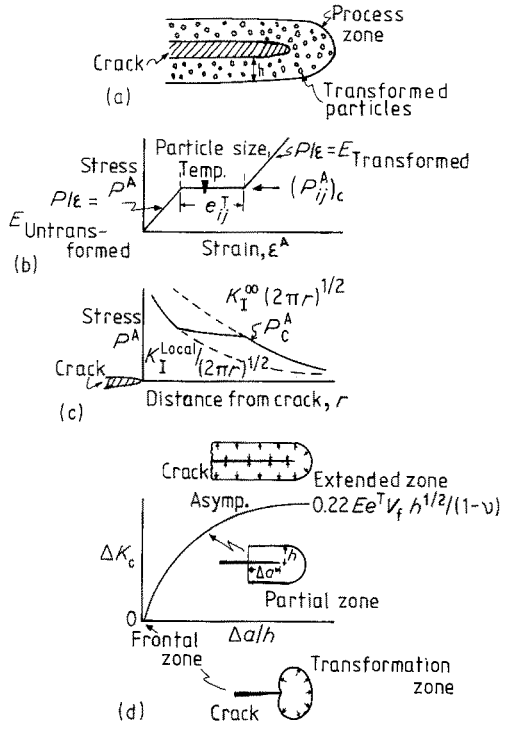


*Figure 1* Schematic drawings illustrating the basis for crack shielding by a transformation zone: (a) the process zone; (b) the stress–strain curve of the transforming materials; (c) the modified stress field ahead of the crack tip; (d) the *R*-curve and the associated transformation zone shapes [15].

crack tip from the applied stress, in a manner analogous to a plastic zone [14, 15, 22, 23]. The characteristics of crack shielding are predicated by the nonlinearity of the stress–strain curve at stresses exceeding a critical transformation stress $(p_{ij}^A)_c$, Fig. 1b. Specifically, upon transformation, the strain exhibits a discontinuity related to the transformation strain, $e_{ij}^T$ [14, 15, 22, 23]. This strain discontinuity is reflected in a corresponding change in the stress ahead of the crack tip within the transformation zone. The crack tip stress is therefore lowered by the transformation, resulting in crack shielding, Fig. 1c, provided that the transformation strain has the same sign as the crack tip strain. On basis of these concepts, the crack-shielding process associated with the transformation in the process zone is most conveniently examined for a dilatational transformation strain, $e^T$.

(i) When the process zone is contained ahead of the propagating crack, i.e. when the crack is embedded in an untransformed solid, the load application results in a frontal transformation zone of dilatational profile, intersecting the crack tip. Integration of the tractions along the transformation zone boundary reveals that $\Delta K_c$, the toughness increment associated with the transformation, is zero. Therefore no toughening occurs.

(ii) When a transformation zone extends fully over the crack surfaces, closure tractions are exerted over the crack surface in addition to the zone-boundary tractions. Integration of these tractions over the transformation zone yields a maximum toughness increment

$$\Delta K_c = 0.21 E e^T V_f h^{1/2}/(1 - \nu)$$

in which $E$ is Young's modulus of the composite, $\nu$ is Poisson's ratio, $h$ is the transformation width, $V_f$ is the volume fraction of the material susceptible to transformation, and $e^T$ is the dilatation strain associated with the transformation.

(iii) When a transformation zone extends partially over the crack, *R*-curve behaviour occurs, $\Delta K_c$ increasing with crack advance, $\Delta a$. An analytic expression with the approximate form of Fig. 1d is given by

$$\Delta K_c \approx \left[\frac{0.44}{\pi(1 - \nu)}\right] E e^T V_f h^{1/2} \tan^{-1}\left(\frac{\Delta a}{h}\right)$$

Two advantages of the model discussed above are: (i) the ability to relate the toughness increment directly to the characteristics of the transformation (volume expansion and shear strain, transformation zone size); and (ii) the ability to explain the *R*-curve behaviour of ZTA, which describes the increase in toughness with increasing crack length [24].

Clarke *et al.* [25] appreciated the existence of the transformation zone and estimated its size as approximately one alumina grain using Raman spectroscopy diffraction (RSD), even though this was the resolution limit of the technique. Ruhle *et al.* [13] estimated, on the basis of HRTEM observation, that the transformation zone was $\sim 5\,\mu m$. It is noticeable that the estimated values are dependent on the techniques used. In addition, the observation of the transformation zone using the various techniques provided indirect evidence for the mechanisms proposed by Rice *et al.* [26, 27] to explain the grain-size dependence of fracture toughness in alumina ceramics [24].

An alternative approach by Lange [5, 28] and Garvie *et al.* [29, 30] was based on a thermodynamic analysis. They considered both the conditions for retaining the metastable tetragonal zirconia particles in the matrix and the toughening increment that can be achieved. The condition for a crack to propagate is a reduction in the total energy of the system, including chemical free-energy associated with the transformation, surface energy, strain energy, and the external applied energy. Their energy balance analysis deduced the existence of a critical size for retention of the metastable tetragonal particles, which implies the possibility of increasing the toughening by controlling the grain size of the constrained zirconia particles. Lange [5] demonstrated that one of the determining factors for toughening is the free-energy change associated with the transformation, $\Delta G$, which could be altered via temperature and the alloy content. Although the transformation zone was considered as one of the factors which influence the toughening, it was assumed to be more or less the inclusion size. In contrast, Ruhle *et al.* [13], using TEM, noted that the transformation zone was $\sim 5\,\mu m$, which was much larger than the inclusion size. On the basis of the Griffith criterion, Lange [5] also concluded that the transformation toughening concept not only resulted in toughening, but also in strengthening of the ceramics.

## 2.2. Microcrack toughening

Microcracks in zirconia-toughened ceramic materials can be subdivided as residual microcracks and stress-induced microcracks [2, 6, 31, 32]. The residual

microcracks are due to the volume expansion and shear strain associated with the tetragonal → monoclinic transformation which takes place on cooling from the sintering temperature [2, 6]. The stress-induced microcracks are those caused by the volume expansion and shear strain associated with the subsequent stress-induced transformation during fracture process [31]. It is considered that residual stresses are required for the formation of stress-induced microcracks; however, the magnitude of the stresses is insufficient to cause spontaneous microcracks. Thus when the external stress and the tensile stress associated with the tetragonal → monoclinic transformation are linearly superimposed on the residual stresses, microcracks will be induced.

The residual microcracks, which have been studied by numerous researchers [2, 6, 33–40], are considered to be the most commonly occurring toughening mechanism in ZTA. With particles larger than the critical size for tetragonal retention during cooling, the zirconia particles transform to the monoclinic phase, and tangential stresses are generated around the transformed monoclinic $ZrO_2$ particles. These, in turn, induce microcracks at the boundaries between the inclusions and the matrix. The microcracks, by their ability to extend in the stress field of a propagating crack, or deflect the propagating crack, can then absorb fracture energy.

In modelling the mechanism, it has been recognized that both the density and orientation of microcracks are two determining factors for the degree of toughening. A similar model to that for the stress-induced transformation toughening has also been developed by Evans *et al.* [9, 11, 14, 41], who deduced from the change in the Young's modulus and dilatation, that microcrack toughening was also a crack-shielding process. Consequently, the toughening is dependent on the development of a process zone at the crack tip.

(i) When the process zone is contained ahead of the crack tip, crack shielding occurs only by virtue of the reduced modulus of the process zone. However, this reduction is largely offset by the reduced crack propagation resistance of the microcracked material within the process zone. Thus the overall toughening is not substantial.

(ii) As with the stress-induced transformation toughening, maximum toughening is achieved when the propagating crack is completely embedded by the process zone. The resultant toughening can be expressed as:

$$\Delta K_c = K_c(0.04f_s + 0.25f_s^2 h^{1/2} E\theta)$$

in which $f_s$ is the saturation density of microcracks, $h$ is the process zone width, $E$ is elastic modulus and $\theta$ is the dilatational strain that results from partial relief of the residual stress by microcracking.

(iii) When the process zone extends partially over the crack length, the toughening achieved can be analyzed in terms of the density of microcracks and the dilatation strain caused by the microcracks.

Again, Evans *et al.* [11] considered the $R$-curve behaviour of the microcracked materials. It is known that the toughening increases with increase in the density of microcracks. However, a too-high density of microcracks can result in a reduction in the fracture toughness, instead of giving toughening [38, 42].

Unlike the stress-induced transformation toughening, the presence of either the stress-induced microcracks or the residual cracks could result in a reduction in the fracture strength, as a consequence of either the presence of subcritical flaws or an increased critical flaw size. The stress-induced microcracks associated with the transformation have been suggested to be the mechanism which controls the limit of strengthening achieved by the transformation toughening mechanism [43, 44]. The failure strength of the stress-induced transformation-toughened ceramic is determined by the critical transformation stress, which refers to the stress required to induce the tetragonal grain to undergo the tetragonal → monoclinic transformation. The link-up or coalescence of the residual microcracks has been shown to reduce the fracture strength significantly [42].

Ruhle *et al.* [45], based on their experimental results, considered the transformation toughening and microcrack toughening as complementary processes in ZTA and showed that both tetragonal and monoclinic zirconia particles in ZTA could give rise to toughening concurrently. In the stress field of propagating cracks, the tetragonal particles could undergo the stress-induced transformation toughening and the residual stresses around already transformed monoclinic zirconia particles could cause microcracks. It was argued that the tetragonal zirconia particles which transformed in the crack-tip stress field did not, however, cause appreciable microcracking. The toughening increments obtained via these two distinct mechanisms were comparable. It was therefore concluded that the highest toughness could be achieved in the composites containing both tetragonal and monoclinic zirconia particles. This conclusion was also supported by the results obtained by Hori *et al.* [46].

## 2.3. Other toughening mechanisms

Other toughening mechanisms considered to operate in ZTA include crack deflection and the formation of compressive surface stresses.

Evans *et al.* [9, 11, 14, 15, 47] considered that cracks can be deflected by localized residual stress fields which are developed as a result of phase transformation, thermal expansion mismatch or by the fracture of a second phase. The deflection results in a degree of toughening dictated by the reduced force on the deflected portion of the propagating crack. For the deflection by a second phase in the matrix, the parameters which have been shown to influence the toughening include volume fraction, particle morphology and aspect radio of the second phase.

Evans and Cannon [9] considered that the nucleation and formation of twins and the loss of coherence associated with the tetragonal → monoclinic transformation could also contribute to the expenditure of energy and result in toughening.

Coyle and Cannon [48] noted the substantial influence of reversibility of the stress-induced tetragonal → monoclinic transformation on toughening. This has also been recognized by Rice [49] and, more recently, by

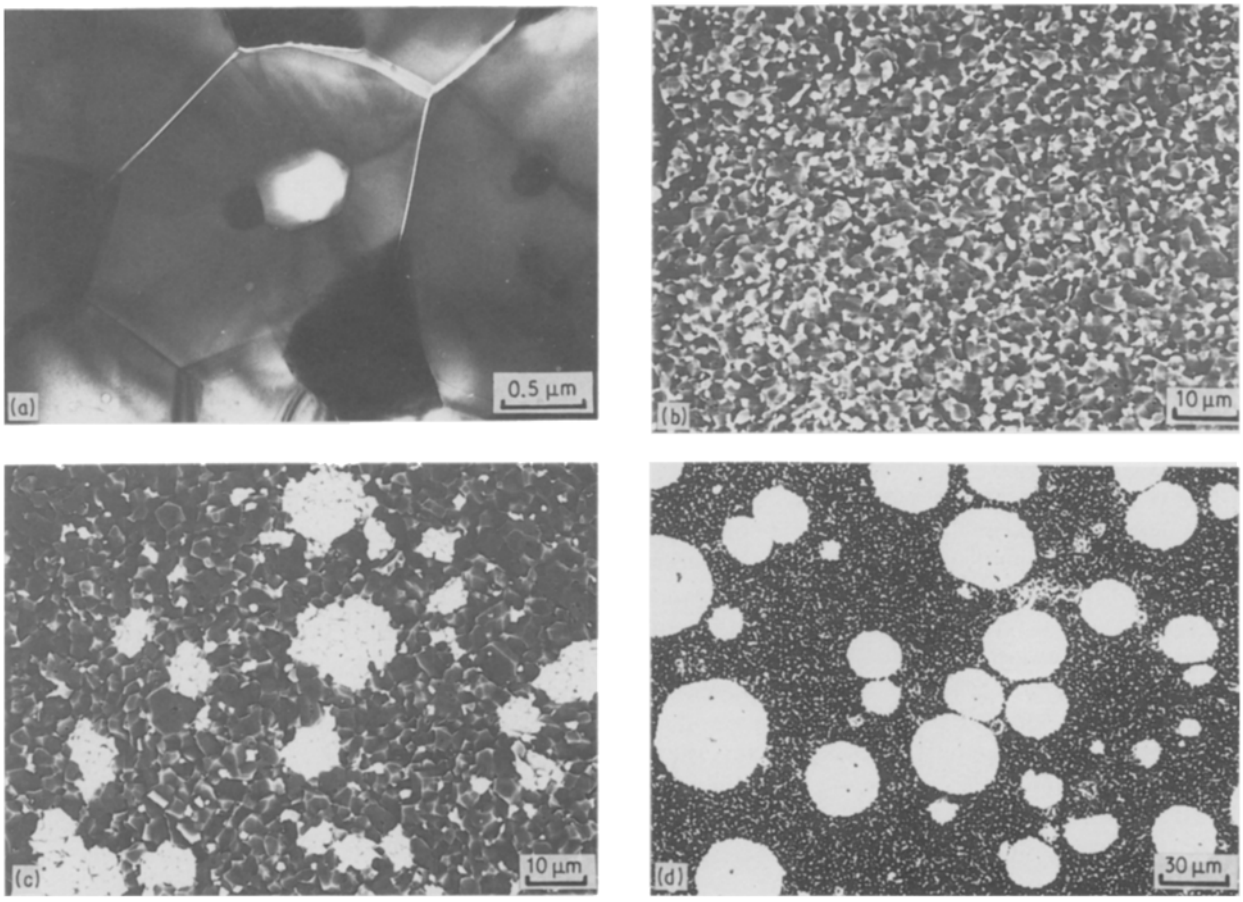


*Figure 2* A transmission electron micrograph showing the microstructure for alumina containing well-dispersed unstabilized zirconia particles. The microcracks at the grain boundaries are due to the volume expansion and shear strain associated with the tetragonal → monoclinic transformation of the dispersed zirconia particles. (b-d) scanning electron micrographs showing the microstructures of aluminas containing well-dispersed PSZ single crystals, TZP agglomerates and alumina-zirconia duplex structured composites, respectively.

Marshall and James [50]. The significance of this effect is the possibility that all of the transformed monoclinic $ZrO_2$ in the entire transformation zone can fully reverse when the applied stress is removed, because the transformed zone is in residual compression.

The compressive surface stresses, which are a result of the compressive strain induced by the volume expansion and shear strain associated with the tetragonal → monoclinic transformation on the surface, is an apparent toughening factor for ZTA. The toughening induced by these compressive surface stresses will also have a positive effect on the fracture strength of the composite. A compressive surface stress of 500 to 1000 MPa has been calculated by Claussen and co-workers [10, 51]. It is estimated that the compressive stresses are concentrated in a depth of only about 20 $\mu$m at the surface [52]. The generation of these compressive surface layers has been achieved using techniques such as grinding [10], impact [53, 54], surface chemical reactions [55] and low-temperature quenching [56].

Evans [57] has also considered and analysed the case in which cracks in a brittle material are impeded by obstacles in the form of a second phase with a greater toughness than the matrix. It is apparent that ZTA could satisfy this requirement.

Finally, it is possible for a crack to be branched by a secondary phase present in the matrix or by associated localized stress fields. Crack branching has been noted by Wang [58] in his study on the ZTA duplex structures, in which large PSZ or TZP agglomerates are dispersed in a matrix of alumina or ZTA.

## 3. Microstructures and mechanical properties

Microstructurally, ZTA can be divided into four groups (Fig. 2):

(I) alumina with dispersed unstabilized zirconia (Fig. 2a);

(II) alumina with dispersed PSZ (Fig. 2b);

(III) alumina with PSZ agglomerates (Fig. 2c);

(IV) alumina-zirconia duplex structures (Fig. 2d);

The mechanical properties of these materials are closely related to their microstructures, each of which exhibits its own combination of toughening mechanisms.

### 3.1. Alumina with dispersed unstabilized zirconia

In 1976, Claussen [2] first reported fracture toughness results for alumina with dispersed unstabilized $ZrO_2$ particles Fig. 3. The composites were fabricated by sintering using commercial alumina and two sizes of unstabilized $ZrO_2$ powders: (i) 0.3 $\mu$m and (ii) 1.25 $\mu$m, as the starting materials. Both a density of microcracks

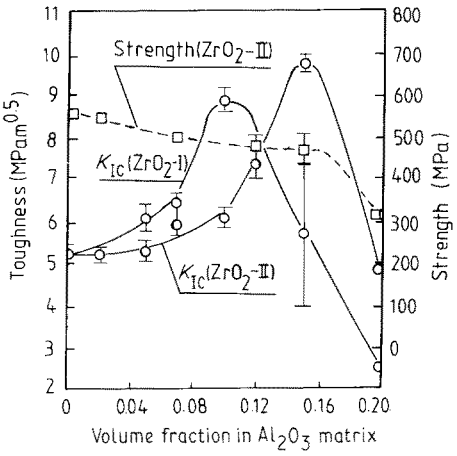


*Figure 3* Fracture toughness and strength of alumina matrix containing unstabilized zirconia particles as a function of the volume fraction of the zirconia additions [2].

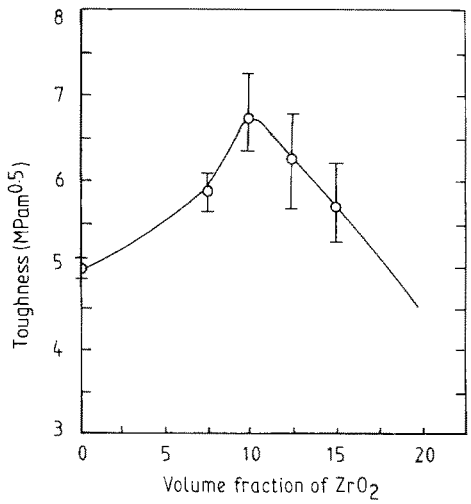


*Figure 4* Fracture toughness of an alumina matrix containing unstabilized zirconia particles as a function of the volume fraction of the zirconia addition, fabricated by Lange using hot-pressing [5].

and tensile stresses were induced by the volume expansion and shear strain associated with tetragonal → monoclinic transformation of the dispersed $ZrO_2$ particles. The extent of the energy dissipation zone was markedly increased by the presence of the induced microcracks. Because of the presence of the induced tensile stresses, certain $ZrO_2$ particles (small sized) could become microcrack formers, limiting the internal flaws to smaller sizes. Therefore, the resulting toughness increase over the samples containing no zirconia was due to the opening and propagation of the microcracks associated with dispersed zirconia particles. Claussen concluded that the fracture toughness could be increased further when uniform, evenly dispersed $ZrO_2$ particles with a diameter slightly greater than the critical value ($D_c$) were used [59].

Later, Claussen *et al.* [60] provided further experimental evidence to support the above mechanisms. They fabricated a composite consisting of alumina and 15 vol % monoclinic zirconia, which was dispersed at the grain boundaries of the matrix. The composite exhibited very high room-temperature fracture toughness (11 MPa $m^{0.5}$) on cooling from 1275° C when microcrack precursors nucleated at $T < M_s$, the tetragonal → monoclinic transformation starting temperature. With increasing time (up to 12 h) at room temperature, toughness and Young's modulus decreased when dilational and thermal expansion strains subcritically propagated intergranular cracks. Thus it was concluded that the toughening of alumina with intercrystalline unstabilized zirconia dispersions is to a great extent caused by microcrack nucleation and extension.

Lange [5] also extensively studied composites consisting of alumina and dispersed unstabilized zirconia. The toughness results of the composites fabricated by hot pressing are shown in Fig. 4. Although he did not give a clear explanation for the results, it is now accepted that toughness enhancement by incorporation of unstabilized zirconia particles with sizes greater than the critical values ($D_c$) in alumina is related to microcrack toughening. The exceptionally low hardness values reported for the composites indicated the presence of a high density of microcracks.

The strength of alumina with dispersed unstabilized $ZrO_2$ particles usually decreases with increasing volume percentage of the $ZrO_2$ added. The explanation given by Claussen *et al.* [2, 3, 59] is that the average flaw size in all composites is increased by addition of $ZrO_2$ particles when compared to pure alumina. It is also suggested that certain flaws are due to an inhomogeneous dispersion of $ZrO_2$ in the composites, i.e. that clustering of the $ZrO_2$ precipitates is taking place.

Green [61] analysed the critical microstructure for microcracking in ZTA. He considered that the internal strains associated with the tetragonal → monoclinic transformation were able to introduce microcracks in the composites. However, the ability of the zirconia particles to transform and therefore to cause microcracks was size dependent. The critical size was affected by thermal treatment and the quantity of the zirconia addition. For ZTA containing more than 7.5 vol % $ZrO_2$, the $ZrO_2$ particles ($\sim 1\,\mu m$) were found to pin alumina grain boundaries, thus limiting the grain growth of alumina grains. Green also considered the mechanical properties of the composites which exhibited microcracks associated with the tetragonal → monoclinic transformation and concluded that microcracks would substantially reduce the fracture strength.

Recently, a criterion for microcrack propagation, which is a determining factor for both the fracture strength and fracture toughness of microcracked ZTA containing high $ZrO_2$ contents (usually > 10 to 15 vol %), has been developed by Wang and Stevens [42] based on the energy-balance approach given by Lange [62]. They considered the opening and consequent stability of cracks associated with the tetragonal → monoclinic transformation in ZTA. The condition for crack opening and propagation was the reduction of the total internal energy of the system. The crack stability and instability were defined as crack arrest and crack extension, respectively. It was shown that the dependence of the microcrack development on the size ($R$) and the degree ($\delta$) of the stabilization of zirconia inclusion could be expressed as

$$C = R\left[\left(1 + \frac{\beta^2\delta^2 R}{K\gamma}\right)^{1/2} - 1\right]$$

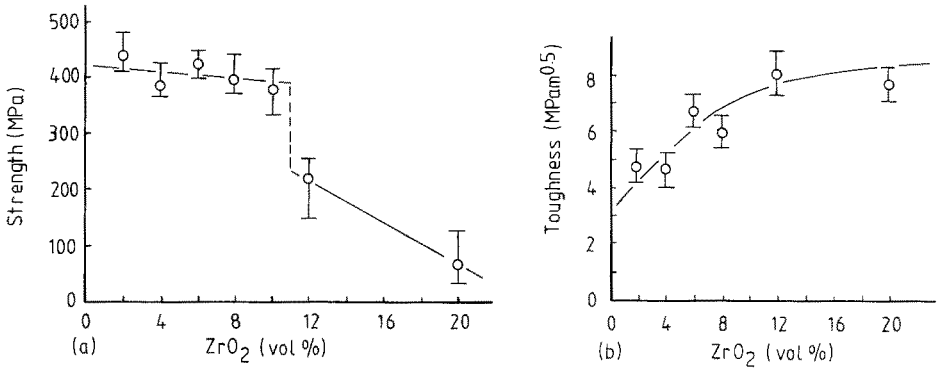


*Figure 5* (a) Three-point bend strength of alumina with well-dispersed zirconia single crystals as a function of the zirconia addition. It is interesting to note that the fracture strength shows a fall at a volume fraction of ~12%. (b) Indentation toughness of the alumina with well-dispersed zirconia single crystals as a function of the zirconia addition. It is important to learn that the toughness increases almost linearly with increasing volume fraction of the $ZrO_2$ addition initially, followed by a slight increase with further increase in the $ZrO_2$ addition.

in which $C$ is the half toroidal crack length around the $ZrO_2$ particle, $\gamma$ is the effective fracture surface energy of alumina, $K$ is the overall reciprocal modulus of the composite, and $\beta$ a constant.

On the assumption that a number of identical zirconia inclusions are dispersed in the alumina matrix, it could be shown that the critical volume fraction of the zirconia addition which causes crack link up or coalescence can be expressed as

$$V_z^c = 0.52\left(1 + \frac{\beta^2\delta^2 R}{K\gamma}\right)^{-3/2}$$

The significance of the equations above is twofold: (i) the size of microcrack generated by the transformed monoclinic $ZrO_2$ particle is dependent on both the particle size and the amount of stabilizing agent present; and (ii) when the volume fraction of zirconia addition of a given particle size is less than the critical value the microcracks are stable and do not coalesce. However, the distance between the microcracks will decrease with increasing volume fraction of the zirconia. When there are many microcracks close together, coalescence occurs spontaneously [42].

The above criterion was supported by the experimental results obtained for alumina containing unstabilized zirconia [42]. Fig. 5 shows the mechanical properties of the composites, as a function of volume fraction of the unstabilized zirconia. Microstructurally, the composites are composed of large alumina grains (~5 $\mu$m) and small zirconia grains (~1 $\mu$m). It is seen that when the $ZrO_2$ addition is less than ~12 vol %, the fracture strength decreases gradually with increasing volume fraction of the unstabilized zirconia. However, there is a dramatic fall in the three-point bend strength at ~12 vol % zirconia addition. It is also apparent from Fig. 5b that the indentation toughness increases rapidly with increasing volume fraction of the $ZrO_2$ for the composites containing low volume fractions. When the zirconia addition is greater than ~12 vol %, further increasing the zirconia volume fraction results only in a slight increase in the indentation toughness.

This analysis is also supported by the results of Claussen *et al.* [6], who fabricated ZTAs containing various grades of zirconia additions with the particle sizes ranging from 1.25 to 5.4 $\mu$m, Fig. 6. They attributed the strength decrease to the inhomogeneous dispersion of zirconia particles which increased the critical flaw size, especially at the high volume fraction of $ZrO_2$. One of the more important observations from Fig. 6 is that the fracture strength decreased suddenly over a narrow range of $ZrO_2$ fraction for each grain size; this is considered to correspond to the critical volume fraction. The indentation toughness as a function of zirconia volume fraction indicates that the over extended microcracks did not give toughening; this was shown as a decrease in the toughness, following the initial increase with the increasing volume fraction of zirconia additions. Another important observation is that the critical volume fraction which causes a fall in the fracture strength is dependent on the particle size of zirconia introduced.

Based on their analysis and experimental support, Wang and Stevens [42] concluded that the stability of microcracks played an important role for both the fracture toughness and strength. Only those stable microcracks, which exist in the composites containing

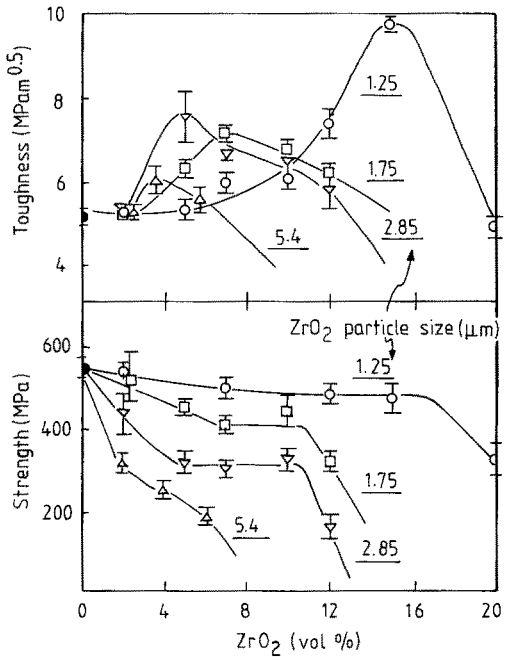


*Figure 6* Fracture toughness and strength results for the composites containing well-dispersed zirconia single crystals fabricated by Claussen *et al.* [6].

low volume fractions of small-sized unstabilized zirconia, provided toughening. The factors which determine the stability of the microcracks included volume fraction of zirconia, its particle size and content of stabilizing agent.

Microcracks in ZTA can also be introduced by a processing step. Noma and Samaoka [63] sintered ZTA composites at a high pressure (6 GPa) and showed that their toughness values were much lower than that for either ordinary alumina or ZTA fabricated by conventional sintering or hot pressing. They considered that the spontaneous cracks caused by the transformation ($ZrO_2$) from the high-pressure phase to the low-pressure phase was responsible for the low toughness. The cracks were observed by SEM and TEM.

An interesting research area for alumina containing unstabilized zirconia is the study of *R*-curve behaviour. Such a study requires an understanding of the microcrack zone and in particular of the effects of density and orientation of microcracks on the dynamic toughening. Recent research includes computer simulation of microcracked microstructures [64].

Becher [65] studied the transient thermal stress behaviour of ZTA. The sizes of alumina and Zirconia grains for his composites which were fabricated by hot pressing were $\sim 5$ and $0.6\,\mu m$, respectively. It was found that the thermal shock resistance, as determined by quench tests, increased with increasing amount of zirconia up to 15 vol %. For composites containing $> 15$ vol % $ZrO_2$ bulk microcracks could become extensive and resulted in a degradation of both the room-temperature properties and the thermal shock resistance.

The mechanical properties of alumina containing unstabilized zirconia at high temperatures have not been extensively studied. The understanding is that the presence of the transformation-induced microcracks will enhance the nucleation and especially the growth of the microcracks and cavitation, which are responsible for the high-temperature failure of ceramics [66, 67].

ZTA offers good thermal properties as a result of the presence of microcracks and zirconia particles, both of which have low thermal diffusivity. Greve *et al.* [68] and Bentsen *et al.* [69] first studied the temperature dependence of the thermal diffusivity of these materials. It was noted that the thermal diffusivity values on heating and cooling above $\sim 1000°$ C were not reproducible, whereas the values below 800° C were. The obvious interpretation is that the diffusivity is affected by the microcracks in the composites. Hasselman *et al.* [70] noted similar results for alumina containing unstabilized particles of $ZrO_2$–$HfO_2$ solid solutions.

There are potential applications for unstabilized zirconia toughened alumina in the refractory industries. The presence of the microcracks results in a useful enhancement of the thermal shock resistance for this class of materials.

### 3.2. Alumina with dispersed PSZ

The dispersion of PSZ particles in an alumina matrix is analogous to the ordinary PSZ ceramic in which tetragonal precipitates exist in a cubic zirconia matrix intergranularly or intragranularly [71, 72]. There has been extensive research into both the fabrication and the mechanical property–microstructure relationship of alumina with dispersed PSZ. The alloy oxides which are used to partially stabilize the toughening agent have been, for the most part, $Y_2O_3$ and $CeO_2$ [5]. A toughness value of 10 MPa $m^{0.5}$ has been reported for material fabricated by conventional sintering.

It was Claussen and Jahn [3] who first reported alumina toughened with PSZ dispersions. The initial study was on the dependence of the mechanical properties on the PSZ volume fraction. Lange [5] subsequently fabricated a series of samples using hot pressing, starting with submicrometre alumina and PSZ powders. The mechanical properties measured on the samples included fracture toughness, fracture strength, Young's modulus and hardness, Fig. 7. A considerable increase in both the fracture toughness and fracture strength is achieved by adding tetragonal zirconia particles into the alumina matrix. The increased fracture toughness is due to the stress-induced transformation toughening of the metastable tetragonal particles. The enhanced strength at the room temperature is due to both the stress-induced transformation toughening and the reduced grain size of the alumina matrix. In contrast, an addition of cubic zirconia particles into the matrix lowers the fracture toughness as a consequence of residual stresses associated with the negative differential thermal expansion and shrinkage of the cubic zirconia particles with respect to the alumina matrix. Both the Young's modulus and hardness of the composites containing PSZ inclusions obey a linear Rule of Mixtures.

Becher [73] considered that there was a critical volume fraction of a given particle size to cause an autotransformation. This concept is based on the fact that an internal tensile stress is generated by the thermal expansion mismatch between tetragonal zirconia and alumina matrix ($\alpha$-$Al_2O_3 = 6.0 \times 10^{-6}\,C^{-1}$; $\alpha$-$ZrO_2 = 10.0 \times 10^{-6}\,C^{-1}$). The internal tensile stress increases with increasing PSZ content in alumina. When the PSZ content is at the critical volume fraction, which generates an internal tensile stress equal to the critical transformation stress, an autotransformation takes place. Becher proved experimentally the existence of the critical volume fraction, which is solute and temperature dependent.

It should be pointed out that the decrease in the fracture toughness when the $Y_2O_3$ content is $< 1$ mol % is due to the spontaneous transformation and therefore a decrease in the amount of the available transformable tetragonal zirconia present in ZTA. The solute dependence of the toughness is affected by the temperature, which influences the chemical driving force for the phase transformation. As shown in Fig. 8, a decrease in temperature will result in an increase in the chemical driving force for the transformation, which is reflected by an increase in the toughness. When the testing temperature is decreased to 78 K, the toughness peaks at a higher $Y_2O_3$ content and a high toughness value is measured.

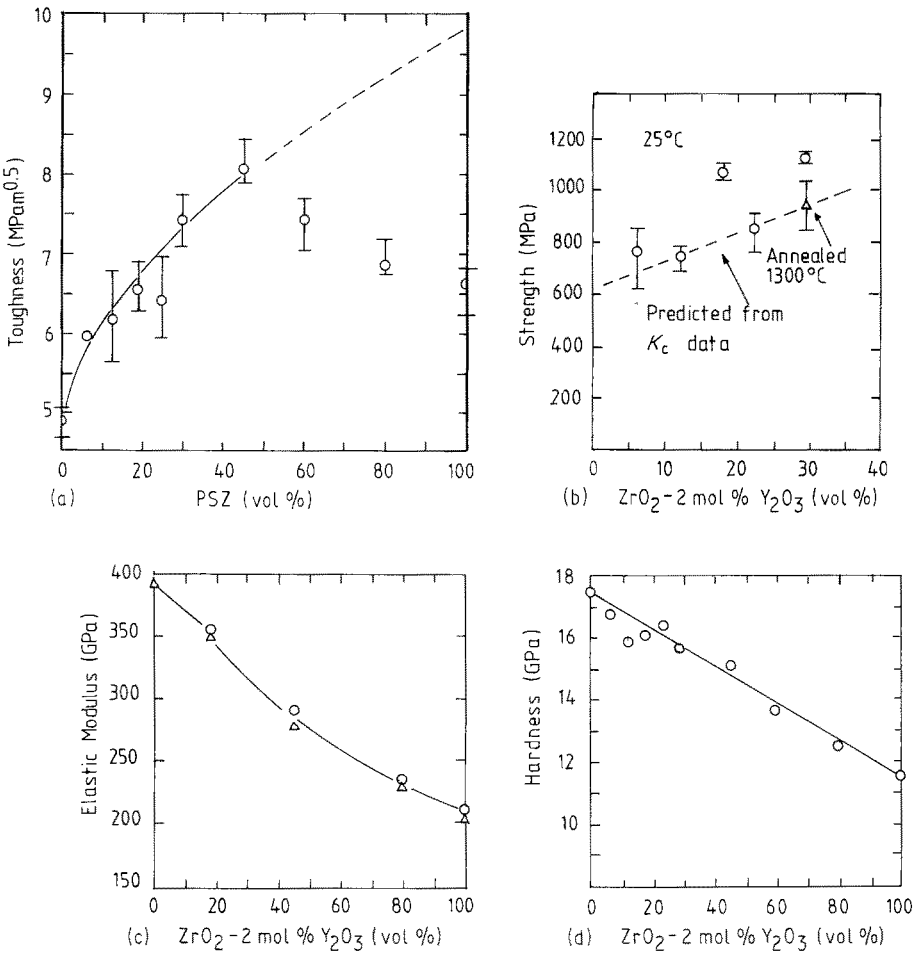


*Figure 7* (a) The dependence of the fracture toughness on volume fraction of PSZ addition for the composites fabricated by Lange using hot pressing [5]. (b) The dependence of the fracture strength on the volume fraction of PSZ addition for the composites [5]. (c) The composition dependence of the elastic modulus for the composites [5]. (○) Extension (60 kHz); (△) flexural (9 kHz). (d) The composition dependence of hardness for the composites [5].

Another factor which influences the microstructure and properties of ZTA is the grain size of the PSZ inclusions. Heuer *et al.* [75] studied the stability of various grain-sized PSZ particles in ZTA with reference to the transformation temperature. The stability could be considered as a measure of the stress required to induce the transformation. Critical factors which affect the size dependence of the transformation temperature include surface and strain energy, the chemical free-energy change of the transformation and the possibility of nucleating the martensitic transformation [76, 77]. A high transformation temperature for large tetragonal zirconia particles will result in a high toughness at room temperature as a result of the enhanced free energy change of the system. Large particles undergo the martensitic transformation more readily than do smaller particles. For example, the transformation starting temperatures for 0.6 and 1.5 $\mu$m particles are 400 and 1000 K, respectively. It is thus apparent that the large tetragonal zirconia particles will offer a more effective toughening than the smaller ones.

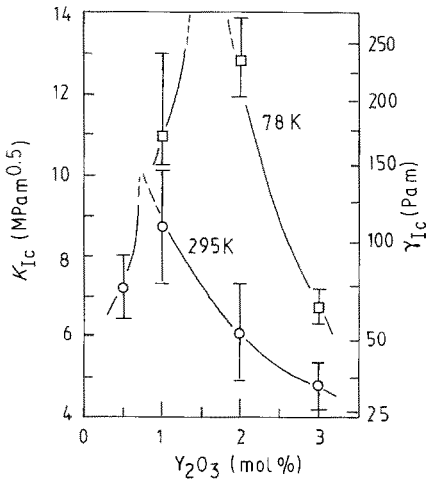


*Figure 8* The dependence of fracture toughness on $Y_2O_3$ content for the alumina containing $Y_2O_3$ partially stabilized zirconia at room temperature and at 78 K. Fabricated by Becher [73].

It is interesting to understand the strength–toughness relationships of alumina containing PSZ single crystals. It is considered that the fracture strength is controlled by the largest flaws present in the structure. From the modified Griffith equation [78], strength should be proportional to the fracture toughness if the processing defects are unchanged. The strength usually reflects the increase in fracture toughness, with the increase in the PSZ content in ZTA [5]. However, the materials which offer the highest toughness are not generally those which offer the highest strength. The materials with the highest strength usually contain slightly more stabilizer than those offering the highest toughness. It has also been suggested that the critical

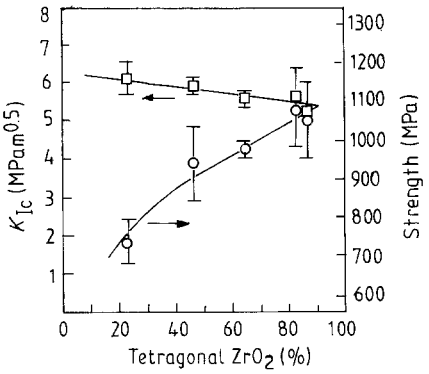


*Figure 9* The dependence of fracture toughness and strength on percentage of tetragonal phase for a composite containing a constant amount of PSZ addition [79].

transformation stress determines the failure strength [43], the transformation-induced microcracks increasing the inherent crack size until it reaches the critical size.

Ruhle *et al.* [79] studied the phase dependence of the mechanical properties for a ZTA containing a constant amount of PSZ addition, Fig. 9. It is apparent that a balance of fracture toughness and strength can be controlled by the percentage of the tetragonal and monoclinic phases in ZTA.

The characteristics of the tetragonal → monoclinic phase transformation in ZTA is of importance. It has been noted that the transformation zone in ZTA is different from that observed in TZP [13]. The transformation in ZTA is a geometrically inhomogeneous process, indicated by the islands of transformed particles some distance from the process zone in ZTA. Angular zirconia particles at grain boundaries or junctions preferentially transform to monoclinic phase on application of an external stress, a consequence of the higher stress concentration developed at the sharp points.

Becher [80] observed improved slow crack growth resistance in alumina containing PSZ dispersions. The contribution to the improved slow growth resistance by the stress-induced transformation toughening was considered to be controlled by the degree of stabilization of the PSZ. Based on his experimental results, Becher confirmed that the stress-induced transformation was a crack-shielding process.

The potential applications for ZTA necessitate a knowledge of the mechanical properties at high temperatures. A thorough study was made by Lange [5] who reported the results shown in Fig. 10. The temperature dependence of the mechanical properties is related to the temperature dependence of the chemical free-energy change associated with the tetragonal → monoclinic transformation. The driving force or the reduction of the free energy for this transformation decreases with the increase in temperature. The transformation toughening ceases to occur at the transformation temperature, as it becomes thermodynamically impossible. This is clearly reflected in the drop in fracture strength and toughness with increasing temperature. On the basis of his experimental results, Lange [5] proposed the following equation to describe the temperature dependence of the fracture toughness of ZTA

$$K_c = A - mT$$

where $T$ is temperature, $A$ and $m$ are constants, respectively.

Li *et al.* [81] measured the temperature dependence of fracture toughness for a ZTA containing 5 vol % tetragonal zirconia using the three-point single-edge notch (SENB) method and noted that the toughness was almost constant at temperatures below 900° C; a fall occurred at temperatures of ~ 1000° C. This was considered to correspond to the phase transformation occurring at this temperature.

It was suggested by Claussen and Ruhle [10] that the microstructures for optimum toughening and optimum strengthening were similar. That is, all of the dispersed PSZ particles should be intercrystalline and uniformly dispersed, of irregular shape and present as a high volume fraction. For the alumina matrix a small equiaxed grain was preferred. In practice, however, it has been found that these requirements are more applicable to fracture strength optimization. High fracture toughness has usually been obtained with intermediate (~ 5 μm) alumina grain sizes [26, 27] and with both tetragonal and monoclinic particles present [45, 46].

Pabst *et al.* [82] and Orange *et al.* [83] investigated the dynamic fatigue and wear resistance of ZTA and discussed the optimum microstructure to balance various mechanical properties. It was found that stress-induced transformation resulted in a decrease in

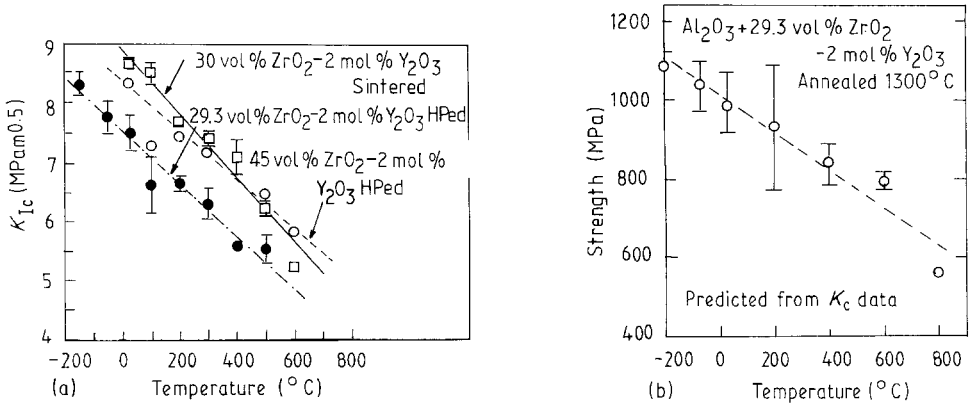


*Figure 10* (a) The fracture toughness as a function of temperature for the alumina–zirconia composites fabricated by Lange using both sintering and hot pressing [5]. (b) Fracture strength dependence on temperature for the hot pressed alumina–zirconia composite [58].

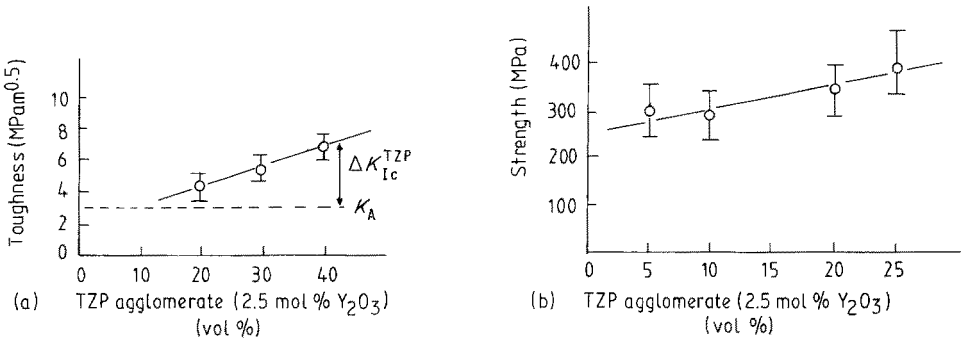


*Figure 11* (a) The indentation toughness as a function of volume fraction of TZP (2.5 mol % $Y_2O_3$) agglomerates for the sintered alumina containing the large TZP agglomerates. (b) The three-point bend strength as a function of the agglomerate addition for the composites [58].

subcritical crack extension velocity and dispersion of pure or stabilized zirconia particles in alumina increased the static fatigue performance of the materials. However, the wear resistance of ZTA was reduced when compared with that of pure alumina. This could be explained by the friction stress-induced transformation on the surface, resulting in microcracks.

It has been found that the composites of Y-PSZ (major-phase, 80 vol %) and alumina (minor phase, 20 vol %), known commercially as super-Z materials and fabricated by hot isostatic pressing (HIPing) using submicrometre powders as the starting materials, exhibit remarkably high fracture strengths (2400 MPa) at room temperature, the highest value reported for zirconia–alumina composites [84–86]. The materials also display a high fracture toughness (17 MPa $m^{0.5}$) at room temperature. The improved mechanical properties at high temperatures are also attractive for engineering applications. Microstructurally, the materials are characterized as a uniform dispersion of $< 0.5\,\mu m$ alumina particles in a fine-grained zirconia matrix ($\sim 1\,\mu m$). Their fractures are mainly intergranular. The high fracture strength could be attributed to the fine-grained structure, which is a consequence of HIPing and the presence of the grain growth-inhibiting second phase. As yet, no plausable explanation has been advanced to account for the mechanical properties in terms of the toughening mechanisms discussed earlier.

## 3.3. Alumina with dispersed PSZ agglomerates

The composites consisting of an alumina matrix and PSZ agglomerates were first fabricated by Evans and Stevens using hot pressing [87, 88]. The microstructure was composed of an alumina matrix and uniformly dispersed large PSZ agglomerates ranging from 5 to $25\,\mu m$ in size with occasional larger agglomerates present. The average grain size of the alumina matrix was $\sim 5\,\mu m$, a small amount of porosity was also present. An indentation toughness of 13.5 MPa $m^{0.5}$ and a strength of 250 MPa were obtained for this composite. The authors compared the structure with the fine-grained ZTA composites for toughness and the submicrometre grain sized ZTA composites for strength. It was suggested that the occasional large zirconia agglomerates together with the large processing defects in the alumina matrix, were responsible for the large flaw size, and hence the low fracture strength. It also suggested that close control of the agglomerate size together with a fine-grained matrix should result in the development of a higher strength without a concurrent decrease in the toughness.

Recently, alumina with larger TZP agglomerates (20 to $50\,\mu m$) was fabricated by Wang and Stevens [58, 89] by conventional milling, mixing and sintering. The mechanical properties of the composites were characterized for the indentation toughness and three-point bend strength, both of which increased almost linearly with increasing volume fraction of TZP agglomerates, Fig. 11. Fabrication and characterization of these composites showed that the fracture toughness due to the different mechanisms could be demonstrated. Two mechanisms were operative in the composites, stress-induced transformation toughening which occurred inside the agglomerates and crack deflection at the interface between the large agglomerates and the matrix.

## 3.4. Alumina–zirconia duplex structures

Although there have been a variety of definitions for these structures, the ZTA duplex structures considered in this group are those containing both zirconia agglomerates and zirconia single crystals in an alumina matrix.

A comprehensive study on ZTA duplex structures has been made by Wang and Stevens [58, 89]. The microstructures were designed to combine the different toughening mechanisms synergetically. Increased toughness could then be achieved by development of a microstructure containing both $ZrO_2$ agglomerates and single crystals. If partially stabilized and unstabilized zirconia particles are dispersed in an alumina matrix, although the dilation from the transformation and microcracks are additive at the transformation boundaries, the lower modulus resulting from the presence of the monoclinic zirconia particles generates a small permanent strain and reduced hysteresis [11]. This lower modulus results in a reduction in the amount of constrained metastable tetragonal zirconia particles compared with in a high-modulus matrix.

If, however, PSZ or TZP agglomerates and unstabilized zirconia particles are introduced into an alumina matrix, the lower modulus of the matrix, caused by the presence of cracks associated with the discrete monoclinic zirconia particles, does not affect the constraint

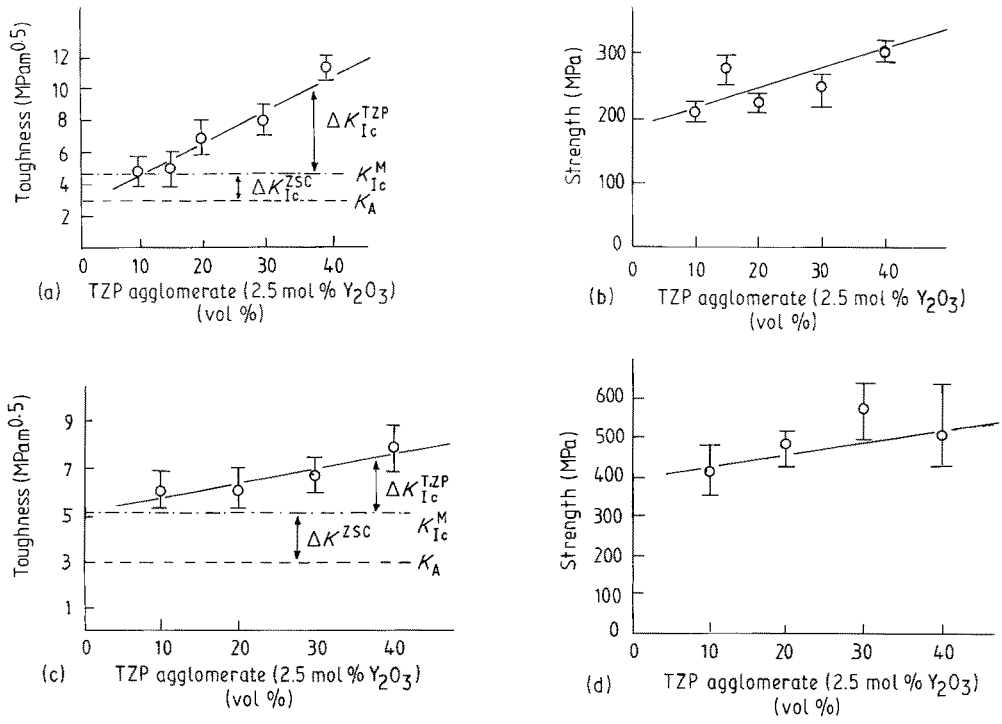


*Figure 12* (a) Dependence of indentation toughness on the volume fraction of TZP (2.5 mol % $Y_2O_3$) agglomerates for the sintered alumina–zirconia duplex structured composites (Table II). (b) The three-point bend strength as a function of the TZP agglomerate addition for the composites [58]. (c) Dependence of indentation toughness on the volume fraction of TZP (2.5 mol % $Y_2O_3$) agglomerates for the hot pressed duplex structured composites (Table II). (d) The three-point strength as a function of the TZP agglomerate addition for the hot pressed composites [58].

on the PSZ or TZP grains inside the agglomerates which remain tetragonal due to their small grain size and mutual constraint. At the same time, the introduction of both large TZP agglomerates (20 to 50 $\mu$m) and monoclinic of PSZ single crystals into an alumina matrix, can result in crack deflection in conjunction with other possible toughening mechanisms, enhancing the toughening increment of the composite.

One of the important steps in fabrication of the duplex structures is retention and uniform distribution of the large PSZ or TZP agglomerates in the matrix. This can be achieved by presintering spray-dried $ZrO_2$ powders, which have a spherical morphology, before mixing with the matrix powder. The mixing can be performed by either a wet or dry process.

The ZTA duplex composites fabricated by Wang and Stevens [58, 89], using conventional sintering and hot-pressing routes can be subdivided into three groups on the basis of whether the zirconia single crystals and agglomerates are unstabilized or partially stabilized, Table I. It is apparent that the toughening mechanisms achieved are dependent on the degree of stabilization of the zirconia inclusions.

Fig. 12 shows two examples of the mechanical properties of the duplex composites, both sintered and hot-pressed, as a function of the volume fraction of TZP agglomerates in the matrices. The microstructure characterizations of these composites are summarized in Table II.

From their experimental results on the ZTA duplex structures, Wang and Stevens established the following trends [58, 89]:

(i) the indentation toughness increases linearly with the volume fraction of either TZP or $ZrO_2$ agglomerates, for both the sintered and hot-pressed specimens;

(ii) the fracture strength of the sintered samples increases in the same manner as the fracture toughness. However, the strength-toughness relationships for the hot-pressed samples are complicated as a result

TABLE I The duplex structured alumina–zirconia composites Wang and Stevens [58, 89]

| Designed structures | Possible mechanisms |
|---|---|
| 1. Alumina with dispersed $ZrO_2$ single crystals and TZP agglomerates (20 to 50 $\mu$m) | Transformation toughening, microcracking toughening and crack deflection |
| 2. Alumina with dispersed PSZ single crystals and TZP agglomerates (20 to 50 $\mu$m) | Transformation toughening and crack deflection |
| 3. Alumina with dispersed $ZrO_2$ single crystals and $ZrO_2$ agglomerates (20 to 50 $\mu$m) | Microcrack toughening and crack deflection |

TABLE II Microstructural characteristics of the duplex structured alumina–zirconia composites (Figs 12 a to d). Matrix composition: alumina + 10 vol % $ZrO_2$ single crystals. Wang and Stevens [58, 89]

| Specimens | Hot pressed | Sintered |
|---|---|---|
| Phases of $ZrO_2$ single crystal | 79 wt % tetragonal 21 wt % monoclinic | 30 wt % tetragonal 70 wt % monoclinic |
| TZP agglomerates | 100 wt % tetragonal | 100 wt % tetragonal |
| Alumina grain size ($\mu$m) | 2 | 4–5 |
| Grain size of the dispersed $ZrO_2$ single crystals ($\mu$m) | 0.5 | 1 |
| Shapes of large TZP agglomerates | Ellipsoidal | Sperical |

of the change in the critical flaw size present in the different materials;

(iii) the indentation toughness is dependent on the volume fraction of the PSZ or $ZrO_2$ single crystals; increased addition of PSZ and $ZrO_2$ single crystals results in an increased amount of stress-induced transformation toughening and microcrack toughening, respectively;

(iv) the fracture toughness of the samples containing TZP–2 mol % $Y_2O_3$ agglomerates is higher than that for the samples containing TZP–2.5 mol % $Y_2O_3$ agglomerates. This is similar to the toughness dependence on $Y_2O_3$ content for TZP ceramics [90];

(v) the fracture toughness of hot-pressed specimens is slightly lower than that of the conventionally sintered specimens.

Wang and Stevens [89] explained their results on the basis of the individual toughening mechanisms operative in the agglomerates and the matrices. The toughness values were broken down into three components, namely the intrinsic toughness of alumina, $K_A$, the toughening by the PSZ or $ZrO_2$ single crystals, $\Delta K_{Ic}^{ZSC}$, and the toughening by the agglomerates, $\Delta K_{Ic}^{TZP}$, Fig. 12.

### 3.5. Comparison of the four structures

As discussed above, the four different-structured ZTAs differ in toughening mechanisms and therefore in the mechanical properties. Stress-induced transformation toughening, compressive surface stresses and crack deflection can all result in both toughening and strengthening [9, 11]. In contrast, microcracked ZTA shows an enhanced toughness and a decreased strength, as a consequence of increased critical flaw size associated with microcrack coalescence during cooling from the sintering temperature or during the fracture process. A more important concept is that microcrack toughening is even a more effective mechanism than stress-induced transformation toughening in ZTA. Microstructurally, a tougher ZTA is achieved when the TZP/PSZ agglomerates are dispersed in the matrix and a stronger one is achieved when PSZ single crystals are dispersed in the matrix.

Structure I shows an increased toughness and a decreased strength as a result of microcracks in the structure. Structures II and III exhibit both increased toughness and strength as a consequence of the stress-induced transformation toughening and crack deflection, respectively. The duplex structure (structure IV, Fig. 2d) shows superior toughness as a result of a combined mechanism, including stress-induced transformation, microcracks and crack deflection. The strength of the duplex-structured ZTA can be increased by careful control of processing parameters to reduce the flaws associated with differential sintering of the large agglomerates with respect to the matrix.

Selection of a specific structured ZTA will be dependent on the specific applications. A tougher and more thermally shock resistant ZTA contains unstabilized zirconia single crystals. A stronger material with moderate toughness contains well-dispersed partially stabilized zirconia single crystals. Hot-pressed duplex structured ZTA offers both the toughness and strength, which are great attractions to engineering applications.

## 4. Fabrication

Like the other engineering ceramics, the fabrication of ZTA is concerned with powder preparation, green forming and the densification processes.

### 4.1. Powder preparation

The following methods have been utilized as powder preparation routes for ZTA.

#### *4.1.1. Mechanical mixing*

Mechanical mixing of alumina and zirconia powders is the most convenient and economic route for powder preparation. It can be classified into wet and dry mixings. The former route can produce a more uniformly dispersed powder, whilst the latter route is usually followed by a milling process to break down any agglomerates which have formed.

Aksay *et al.* [91] studied the dispersion states of aqueous alumina/zirconia colloidal suspensions by measuring the particle size distribution as a function of pH value. They showed that mutual dispersion was achieved at pH values of 2 to 3.5. The consolidated composites formed by the colloidal filtration reflected the uniformity of the colloidal state. The mean flexural strength (896 MPa) of the sintered composites dispersed by the colloidal suspension was 1.6 times that of the bodies consolidated by isostatic pressing.

#### *4.1.2. Sol–gel processes*

When the individual components are mixed in the form of sols, for example, aluminium nitrate, zirconium oxychlorate, zirconium acetate, a good $ZrO_2$ dispersion in alumina is obtained after calcination. However, large quantities of powders are usually difficult and expensive to prepare.

Pugar and Morgan [92] obtained an extremely uniform dispersion of alumina containing 10 vol % zirconia by heating an amorphous precursor, an Al/Zr co-polymerized alkoxide network structure. It was also noted that during crystallization, the grain growth of the $ZrO_2$ was coupled to the $\gamma$–$\alpha$ phase transformation of alumina.

Hideyuki *et al.* [93] prepared alumina–zirconia powder by spraying an alcohol solution containing 20% Zr–Al-organometallic compounds, followed by calcining at 800° C. Yoshimatsu *et al.* [94] used a similar method to obtain balloon-like particles, with the particle size being in the range 0.5 to 2 $\mu$m. The resulting powders contained a high fraction of tetragonal zirconia.

Murase *et al.* [95] prepared the well-dispersed powders by adding $NH_4OH$ to hydrolysed zirconia sols containing various amounts of aluminium sulphate, to obtain a mixture of ultrafine monoclinic zirconia and aluminium hydroxide. The mixture was then heat treated at temperatures between 500 and 1300° C to decompose the hydroxide.

Debsikdar [96] systematically studied the influence of synthesis chemistry on alumina–zirconia powder characteristics. Three different chemical processes

were employed to synthesize $Al_2O_3$–20 wt % $ZrO_2$ powders: (i) chemical polymerization; (ii) destabilization of mixed sols; and (iii) coprecipitation. The particle size of the powders produced was of the order of 1.5 to 3.0 nm, which appeared amorphous using electron diffraction. It was shown that the physiochemical characteristics and crystallization behaviour of these chemically derived powders were significantly influenced by the chemistry of the powder synthesis. The powder produced by the chemical polymerization and the colloidal processes retained the tetragonal phase completely after calcining at 600° C, but significant transformation of the tetragonal to monoclinic zirconia occurred in the coprecipitated powder under identical conditions. Furthermore, the 1550° C calcined powder derived from the chemical polymerization process retained a substantial amount of tetragonal zirconia even after annealing at 1000° C for 72 h.

#### 4.1.3. Partial chemical methods

The use of high-quality alumina or zirconia powders, together with sols of zirconium or aluminium compounds, respectively, yield uniform particle distributions after decomposition of the sols. Wang [58] developed well-dispersed alumina–zirconia powders by mixing alumina powder and $Zr[NO_3]_4 \cdot 5H_2O$ in propanol, followed by drying and thermal treatment at 550° C. Sproson and Messing [97] achieved well-dispersed powders by decomposing alumina–$ZrO[NO_3]_2$ slurry in an EDS furnace at 1000° C, using an atomizer air pressure of 138 KPa and a solution flow rate of 4 ml $min^{-1}$. The dispersed powder made in this way contained tetragonal zirconia particles.

Fegley *et al* [98] prepared well-dispersed powders by controlled hydrolysis of zirconium propoxide in an anhydrous ethanol solution containing α-alumina dispersions. TEM indicated the existence of a fluffy zirconia coating on the individual alumina particles.

#### 4.1.4. CVD process

Alumina–zirconia powders can be obtained via CVD reactions by feeding a mixture of gaseous aluminium and zirconium compounds into an $H_2/O_2$ flame. The resultant powders show an average particle size ranging from 40 to 50 nm [99].

Kagawa *et al.* [100] prepared alumina–zirconia powders by spraying their corresponding nitrate solutions into an inductively coupled plasma (ICP) at ultrahigh temperatures (> 2000° C). The resultant powder was composed of metastable tetragonal zirconia and α-alumina. On calcining, the metastable tetragonal zirconia was retained up to 1200° C. At 1280° C the tetragonal zirconia transformed to monoclinic on cooling to room temperature. It was also noted that the amount of the transformed monoclinic zirconia decreased with increase in alumina content, indicating stabilization of the tetragonal zirconia by alumina. This could be explained in terms of the retardation of the grain growth by the presence of alumina particles.

#### 4.1.5. Rapid solidification

Claussen *et al.* [101] performed the rapid solidification of ZTA ceramics by melting and rapidly solidifying the eutectic compositions of $Al_2O_3$ and $ZrO_2$ by means of shock-wave quenching, flame-pressure and high-pressure water atomization. The rapid solidification resulted in amorphous particles, which, on annealing, crystallized at 1310° C. Microcrystalline particles with tetragonal $ZrO_2$ disturbed in an E-$Al_2O_3$ matrix formed at a lower quenching rate. The E-$Al_2O3$ transformed to A-α-$Al_2O_3$ on annealing at 900° C. Echigoya *et al.* [102–104] prepared and characterized unidirectionally solidified ZTA eutectic prepared by the floating zone melting technique. They showed that the fracture toughness of the eutectic was orientation dependent. Maximum toughness values of 9 and 7.5 MPa $m^{0.5}$ were obtained in directions perpendicular and parallel to the solidification axis, respectively.

#### 4.1.6. Hydrothermal oxidation

Recently, $ZrAl_3$ and $Zr_5Al_3$ alloys have been used as starting materials to prepare mixed alumina–zirconia powders by hydrothermal oxidation [105, 106]. Because zirconium and aluminium atoms are distributed on their respective crystallographic positions of the intermetallic compounds, the experiment is expected to result in the fine dispersion of alumina–zirconia powders. It was found that the sizes of the respective oxides were less than those of the $Al_2O_3$ and $ZrO_2$ powders obtained by the hydrothermal oxidation of aluminium and zirconium metals separately [105]. This reduction in particle size was considered to be due to the retarding effect of the alumina particles on the growth of the zirconia particles.

#### 4.1.7. Wear of $ZrO_2$ milling media

Claussen and Ruhle [10] suggested that fine particle dispersion could be obtained by an extensive milling of alumina powder using $ZrO_2$ milling media. The specific surface area of the resultant $ZrO_2$ powder was determined to be $> 100\,m^2\,g^{-1}$. The volume fraction of zirconia was controlled by the milling time in this technique.

### 4.2. Forming methods

Forming methods for ZTA include die pressing, isostatic pressing, tape casting [107] and slip casting [108]. Die pressing and isostatic pressing, which are standard techniques in fabrication of engineering ceramics, have been described in the literature and textbooks. Tape and slip casting of ZTA, which contains two distinct phases with quite different densities ($\varrho_{Al_2O_3} = 3.97$, $\varrho_{ZrO_2} = 6.0$), are considered to be more difficult than those of the single-phase materials. Requena *et al.* [108] slip cast alumina containing monoclinic zirconia both in an acid medium using HCl as deflocculant and in a basic medium using an organic surfactant (Dolapix PC-33). They observed that slip casting in an acid medium resulted in an almost theoretically dense, homogeneous microstructure and a toughness value of 7 MPa $m^{0.5}$ after sintering. In comparison, casting with a basic slip, especially in the presence of sodium

hexametaphosphate, resulted in a less homogeneous microstructure and a toughness of $< 6\,MPa\,m^{0.5}$.

## 4.3. Densification processes

The densification of ZTA has been achieved mostly by hot-pressing (HPing), hot isostatic pressing (HIPing) and pressureless sintering. Other fabrication methods (such as, microwave sintering) have also been reported [109].

### *4.3.1. Sintering*

The sintering of ZTA is believed to occur by a solid-state sintering process, which is evidenced by the phase relation in the alumina–zirconia system [7].

Hsuch *et al.* [110] overviewed the microstructure development during final/intermediate stage sintering, with emphasis on pore/grain boundary separation. Their phenomenological analysis was essentially based upon an interaction of a boundary with a rigid second-phase particle. Their analysis is applicable to the case of ZTA. It has been confirmed that zirconia inclusions in ZTA inhibit both the grain growth of the alumina matrix and the sinterability [111–114].

Lange and co-workers [112–118] extensively studied the sintering of ZTA composites. He first [112] showed that crack-like internal surfaces were present at the fracture origins of the sintered specimens. These surfaces were developed as a result of differential sintering of the agglomerates relative to the surrounding powder compact. Later, Lange *et al.* [115] further considered two kinds of internal crack-like surfaces; tangential and circumferential cracks around hard and soft agglomerates, respectively. It was shown that the low green-density regions sintered faster than the high density agglomerates, although the high-density agglomerates reached end-point density first. Regions containing low green density agglomerates produced circumferential crack-like voids at the agglomerate/matrix boundaries. Regions containing higher green density agglomerates than the matrix were subjected to compressive strains by the matrix and even produced agglomerate motion when the resulting stress field was nonsymmetric. For the composites containing large zirconia agglomerates (e.g. in the duplex structures), the agglomerates shrank away from the consolidated matrix during sintering, producing crack-like internal surfaces around the agglomerates, Fig. 13.

From the viewpoint of mass transportation, Lange *et al.* [117] confirmed that the $ZrO_2$ inclusions exhibited sufficient self-diffusion to move with the alumina four-grain junctions during grain growth. Thus the inclusions exerted a dragging force at these junctions, limiting grain growth of the alumina matrix. Abnormal grain growth occurred when the distribution of the inclusions was not sufficiently uniform to hinder the growth of every alumina grain. In their discussion, Lange *et al.*, compared the $ZrO_2$ inclusions to pore/grain size phenomenon and suggested that the inclusions in alumina would mimic the behaviour of pores in all ways except that pores could be removed by mass transportation, whereas the inclusions could not.

Kraus-Lanteri *et al.* [119] studied the microstructure of the incoherent $ZrO_2/Al_2O_3$ interface of intragranularly located $ZrO_2$ using HRTEM, which provided atomic level information on the interfacial structure. Both ledge-like images and misfit dislocation-like images were observed to accommodate the lattice misfit, depending on the orientation of the interfaces. It was noted that the faceted particles implied at least one low-energy interface.

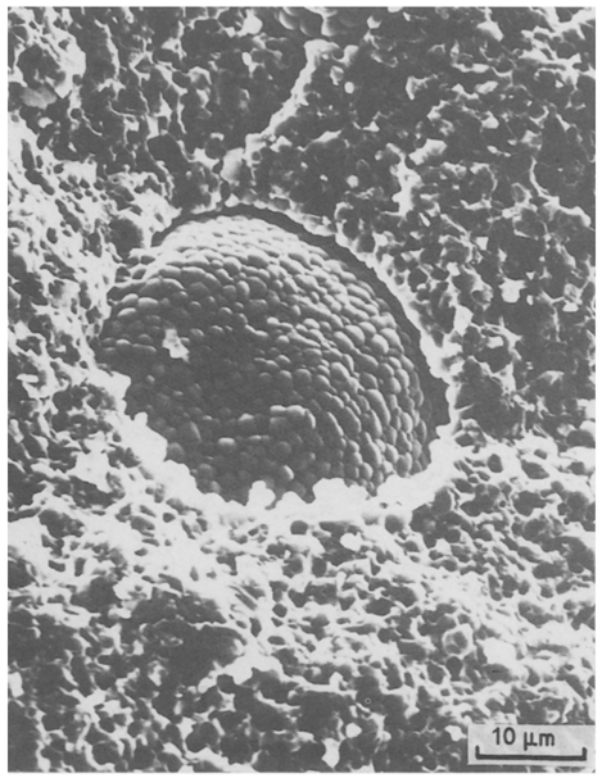


*Figure 13* A scanning electron micrograph showing the large defect which is due to the differential sintering of a large TZP agglomerate with respect to the matrix.

Kibbel and Huer [120, 121] described the two kinds of $ZrO_2$ particles existing in ZTA as faceted intergranular $ZrO_2$ particles located between alumina grains (generally at the grain corners) and spherical intragranular $ZrO_2$ particles, which were located within the alumina grains. The intergranular particles were generally larger than the intragranular particles. They suggested that the large intergranular particles were related to the faster coarsening kinetics associated with the grain boundaries. For the sintering of ZTA, zirconia particles could ripen by two possible processes, i.e. Ostwald ripening or coalescence during the later stages of sintering. During Ostwald ripening, large particles grow at the expense of small ones, a consequence of the variation of solubility with particle size. For coalescence, $ZrO_2$ particles grow as a result of being dragged together by migrating alumina grain boundaries. In this process, grain growth and the disappearance of small alumina grains caused particles to meet, coalesce, and thus formed larger particles, Fig. 14.

Based on their experimental observations, Kibbel and Heuer [120, 121] concluded that the grain growth of intergranular $ZrO_2$ particles in the polycrystalline alumina appeared to occur by coalescence, as particles were dragged by migrating $Al_2O_3$ grain boundaries, and obeyed an $r \propto t^{0.25}$ law. The ultimate rate-controlling process for such coarsening was the rate at

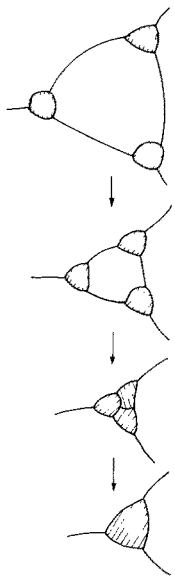

*Figure 14* A drawing showing how $ZrO_2$ particles grow as a result of being dragged by migrating alumina grain boundaries during coalescence [121].

which an individual $ZrO_2$ particle could migrate. This was dependent on the interfacial $ZrO_2$–$Al_2O_3$ diffusion kinetics. On the other hand, the intragranular particles coarsened at a much slower rate which was still dominated by interfacial diffusion kinetics. This led to growth kinetics much slower than an $r \propto t^{0.5}$ or $r \propto t^{0.25}$, at Ostwald ripening law and also to denuded zones adjacent to alumina grain boundaries.

Lange [117] also observed and discussed the microstructures of the ZTA, showing that the $ZrO_2$ particles were primarily located at four-grain junctions which was believed to be due to the strong self-diffusion of $ZrO_2$, although some small $ZrO_2$ grains became relocated within some large alumina grains and had a spherical geometry. It was suggested that this phenomenon appeared to occur by the growth of groups of alumina grains, constrained by relatively few $ZrO_2$ particles, into a single large grain which then "swallowed up" surrounding alumina and zirconia particles. Within regions containing only abnormally large alumina grains, the zirconia grains were ten

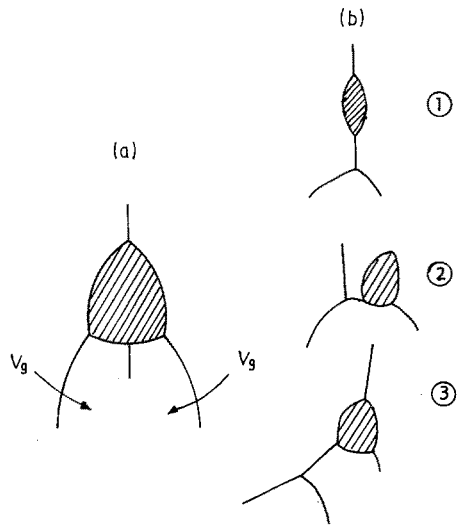


*Figure 15* Schematic drawings showing (a) arrowhead shape of inclusion being dragged along with a three-grain junction and (b) observed breakaway configurations [117].

times smaller than the alumina grains. Lange also noticed various drag/breakway configurations, including $ZrO_2$ grains near three-grain junctions and at two-grain boundaries; a schematic diagram is shown in Fig. 15.

The grain-growth hindrance in ZTA is mutual during sintering, i.e. grain size of both the alumina and zirconia is reduced compared with single-phase alumina or zirconia materials. The retarding effects of alumina particles on the grain growth of zirconia, and therefore on the phase transformation has been well documented in the literature. The zirconia particles in chemically prepared alumina–zirconia powders were found to be more resistant to transformation [96]. The retarding effects of zirconia grains on grain growth of the alumina matrix were clearly observed by Lange *et al.* [117], though it was observed to be composition and size dependent. Grain-growth control was achieved when a majority of four-grain junctions contained zirconia particles. This required the presence of $> 5$ vol % $ZrO_2$ inclusions, which needed to be well dispersed and of fine size. Hori *et al.* [122] noted that grain growth of alumina at 1550° C could be suppressed effectively by addition of $> 1$ wt % $ZrO_2$ which had a particle size of 0.25 $\mu$m.

Recently, Lange and Hirlinger [123] studied the effect of alumina inclusions, with a greater average size (0.6 $\mu$m) than the average particle size of the major $ZrO_2$ phase ($< 0.1$ $\mu$m), on grain growth by sintering the composites at 1400° C and heat treating at temperatures up to 1700° C. The inclusions appeared to have no effect on the grain growth until the zirconia grain was 1.5 times the average inclusion size. Grain-growth inhibition then increased with the volume fraction of the alumina inclusions. It was observed that the inclusions were relatively immobile and most were located within the zirconia grains for volume fractions $< 20\%$ at temperatures $< 1600°$ C. At higher temperature, the inclusions could move with the grain boundaries and coalesce resulting in reduced grain-growth inhibition and a larger average grain size.

It is worth mentioning here that the sinterability of ZTA composites is dependent on the powder processing route. Koh *et al.* [124] reported that plasma-synthesized alumina–zirconia powder sintered much more readily than the pure $Al_2O_3$ powder prepared using similar means.

Lange *et al.* [125] summarized the strength dependence of ZTA on processing steps and indicated that progressive incremental strengthening could be achieved by examination of the fracture surface to identify the inhomogeneity at the fracture origins and thus relate the inhomogeneity to a processing step. The development of a new method that has a high probability of eliminating the strength-degrading inhomogeneity could then be undertaken, Fig. 16.

As discussed earlier, crack-like voids could be induced by large agglomerates in dry-pressed compacts after conventional sintering. Wet milling and colloidal consolidation could eliminate the large soft agglomerates which are broken down and dispersed with surfactant during these treatments. The strength of colloidally consolidated specimens is then determined

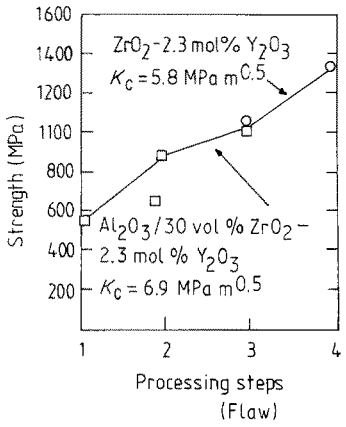


*Figure 16* The dependence of fracture strength of zirconia-toughened alumina composites on the processing step [125]. 1, Dry press; 2, colloidal consolidation; 3, sedimentation; 4, organic burn-out.

by the defects caused by hard agglomerates greater than $\sim 1\,\mu m$, which could be eliminated using sedimentation methods. However, the fracture strength of such treated specimens is still much lower than the expected values as a result of presence of irregularly shaped voids in the structure, which have been suggested to be produced by burn-out of organic inclusions. The organic inclusion related voids could be eliminated by carefully controlling their burn-out during sintering. It is common practice to pre-sinter the green compacts at low temperatures (500 to 800° C) for an extended period of time (5 to 10 h).

The addition of about 1000 p.p.m. MgO to $Al_2O_3$, followed by sintering, resulted in almost 100% dense materials [126]. Similarly, the addition of a small amount of MgO to ZTA has been observed to be effective for sintering and microstructural evolution. In ZTA, $ZrO_2$ is usually not regarded as a higher-valence additive to the alumina. If MgO is added to these composites, however, two major effects will be expected:

(i) a combined effect of MgO and $ZrO_2$ on the densification;

(ii) possible stabilization of incorporated $ZrO_2$ particles by MgO.

A systematic study on MgO addition into ZTA has been made by Kosmac *et al.* [127]. The experimental results given by the authors suggested that:

(i) small additions of MgO to ZTA had an effect similar to that in pure alumina, e.g. the highest densities were obtained when $\sim 1000$ p.p.m. MgO was added, further MgO addition up to 5000 p.p.m. decreased the density slightly Fig. 17;

(ii) the optimum addition ($= 1000$ p.p.m.) was relatively independent of the $ZrO_2$ addition for the levels investigated (up to 30 wt %). The presence of $ZrO_2$ in ZTA apparently led to an increased solubility of MgO in $Al_2O_3$;

(iii) the MgO addition preferentially dissolved in the $Al_2O_3$ then subsequently formed spinel before significant amounts of MgO dissolved in the $ZrO_2$ particles;

(iv) strength and fracture toughness of ZTA were dependent on the level of MgO addition only insofar as the MgO additions modified the grain size and density of ZTA.

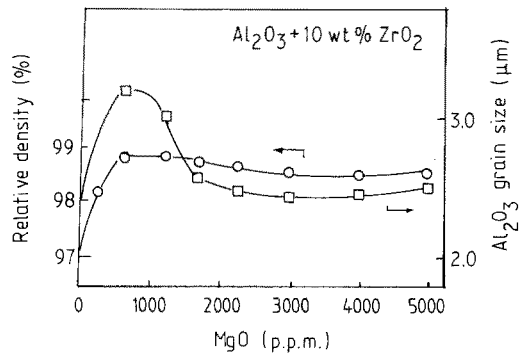


*Figure 17* The effects of MgO sintering aid on the densification and grain size of alumina in zirconia-toughened alumina composites [127].

In a similar investigation, Osendi *et al.* [128] introduced $TiO_2$ into ZTA and noted the following phenomena:

(i) both the initial sintering rate and grain size of the alumina were increased;

(ii) grain growth kinetics of zirconia inclusions increased with annealing at 1570° C. They also observed that toughness varied with the thermal treatment which resulted in a change in the number of transformable tetragonal zirconia inclusions.

Recently, $Na_2O$ and $SiO_2$ additions to ZTA have been made by Yang and Stevens [129], the results indicating that the structures can be influenced by the additions, notably that the shape of the zirconia particles can be modified.

### 4.3.2. Hot pressing

Although the densification of ZTA has been largely achieved by hot-pressing routes, the actual densification processes have not been investigated in detail. One of the advantages of hot pressing over pressureless sintering is the avoidance of differential sintering which is considered to be critical for control of the final microstructure and hence the mechanical properties. On the other hand, the applied pressure during the hot pressing can lead to a build up of residual stresses which influence the tetragonal → monoclinic transformation and can result in less isotropic properties.

The method currently used is to hot press ZTA in graphite dies. The colour of the hot-pressed ZTA changes from a light grey to black as the zirconia volume fraction increases. A colour gradient also exists within the hot-pressed pellets, darker on the outside, light near the centre. The colour is related to the oxygen deficiency of the zirconia inclusions, which lose oxygen in the reducing atmosphere associated with the graphite dies. A white appearance for the hot-pressed specimens can be achieved by thermally treating them at 1200 to 1400° C in air or oxygen for an appropriate period of time (20 to 30 h).

Another commonly observed phenomenon in the hot-pressing of ZTA in graphite dies is the formation of surface cracks. A suggestion made by Lange [5] is that it is due to the volume change of the zirconia particles associated with the oxygen deficiency gradient, because oxygen-deficient $ZrO_2$ has a smaller molar volume [130].

### 4.3.3. Hot isostatic pressing (HIPing)

Lange [5] reported that HIPing could improve the fracture strength of alumina-rich ZTA. Tsukuma *et al.* [85–87] used HIPing to fabricate $ZrO_2$-rich ZTA. Their results can be summarized as follows:

(i) the strengths of HIPed ZTA are much higher than those of the sintered ZTA at room temperature;

(ii) HIPed ZTA exhibits improved strength at high temperatures;

(iii) flaws responsible for fracture of the HIPed ZTA are low-density regions, which are compared with the crack-like internal surfaces responsible for fracture of the sintered samples;

(iv) the size of defects in the HIPed ZTA ($\sim 10\,\mu m$) is much smaller than that in the sintered specimens (50 to 500 $\mu m$);

(v) an advantage of the ZTA fabricated by HIPing over those fabricated by hot pressing is that the microstructure and therefore the mechanical properties are more isotropic and uniform.

Two distinct HIPing processes have been reported for fabrication of ZTA: direct HIPing of as-formed compacts, and post-sintering of pre-sintered specimens by HIPing.

Hori *et al.* [131] studied both the microstructure and properties of HIPed ZTA and found that the tetragonal zirconia particles become more resistant to stress-induced transformation. This could account for the slightly lower fracture toughness of the HIPed specimens compared with those of the sintered specimens. It was also noted that a residual tensile stress occasionally remained in the surface of HIPed ZTA.

## 5. Future aspects

Swain *et al.* [132–134] have attempted to estimate the limit for the maximum strength obtainable by zirconia-toughened ceramics. Their work was based on a recent observation indicating an abnormal relationship between the strength and the toughness in both magnesia and yttria-PSZ. His suggestion was that the stress required to initiate the tetragonal → monoclinic transformation might control the maximum strength. Another mechanism [134] was that the inherent *R*-curve behaviour of these materials limited the strength.

Claussen *et al.* [135, 136] has considered that ZTA represents a new class of high-performance ceramics with spectacular high strength at low and intermediate temperatures (< 700° C). However, at temperatures above 700° C, these tough oxide ceramics, when compared with the two current competitors, SiC and $Si_3N_4$, can no longer be used as load-bearing engineering parts because of the characteristic deficiencies associated with the tetragonal → monoclinic transformation, Fig. 18. Another deficiency in the thermomechanical properties of certain $ZrO_2$-based ceramics is the strength degradation when aged at low temperatures in the range from 150 to 500° C [137, 138].

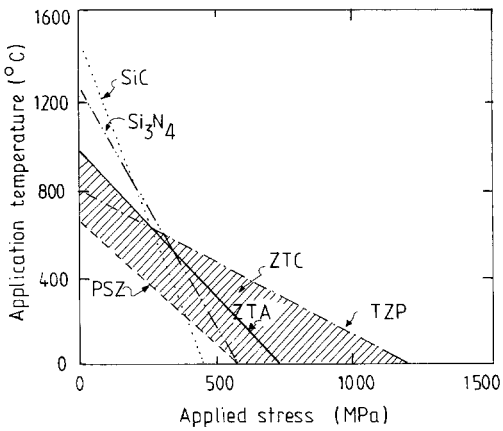


*Figure 18* A drawing indicating the potential application range of some engineering ceramics: $ZrO_2$-toughened ceramics, SiC and $Si_3N_4$ [135].

Claussen [135, 136] has discussed strategies for the microstructural design for high-temperature $ZrO_2$-toughened ceramics, as shown in Table III.

For ZTA, microstructure strategies 7 and 8 have been extensively researched, whilst some of the others are also currently being investigated.

Dispersing an oxide phase such as $Cr_2O_3$, mullite and spinel, or a non-oxide, such as SiC, $Si_3N_4$, TiC, TiN, and $B_4C$ [139–142] into ZTA has been examined because of the technological simplicity. Rather promising improvements have been obtained. At the moment, most of these experiments have been directed toward improving the toughness and strength at intermediate temperatures; however, some comparable improvements have been observed in the high-temperature performance.

Another strengthening method is to introduce $HfO_2$ into $ZrO_2$ inclusions to form Zr–Hf–$O_2$ solid solutions [143, 144] which have higher tetragonal → monoclinic transformation temperatures than for the pure $ZrO_2$ (strategy 4) [145]. The mechanism behind this strengthening method is to disperse the high-temperature toughening agent into the matrix, and therefore to enhance the high-temperature mechanical properties. Although the theoretical transformation temperatures are higher for the Zr–Hf–$O_2$ solutions, the smaller

TABLE III High-temperature microstructural design strategies of $ZrO_2$-toughened ceramics [135, 136]

| Strategies | Experimental approaches |
|---|---|
| 1. Prevention of glassy intergranular phases | Grain-boundary crystallization; reduction of grain-boundary wettability; hot isostatic pressing in an oxidizing atmosphere |
| 2. Special grain-boundary design | Sliding resistant grain-boundary geometry; grain-boundary pinning by hard particles |
| 3. Directional grain growth | Controlled crystallization of plastically deformed materials |
| 4. Increase in $M_s$ * | $HfO_2$ alloying |
| 5. Retention of compressive surface stress | $HfO_2$ surface anneal; surface destabilization. |
| 6. Recipitation hardening | Solution sintering followed by ageing |
| 7. Dispersion strengthening | Addition of hard and high Young's modulus phases |
| 8. Fibre or whisker reinforcements | Introduction of fibre or whiskers of SiC, $Al_2O_3$, etc. |

*$M_s$ = the starting temperature of the tetragonal → monoclinic transformation on cooling.

volume expansion and shear component associated with the transformation for the solutions, compared with those for pure zirconia, limit their potential application as a high-temperature toughening agent.

Although fibre or whisker reinforcement of ZTA is now widely assumed to be the best option for effectively enhancing the high-temperature properties [146], the specific requirements [49] for whisker or fibre reinforcement of ceramic matrices limit the number of useful fibre or whisker-ZTA combinations. The fibres or whiskers which have been used to reinforce ZTA at present include SiC whiskers, $Si_3N_4$ fibre or whiskers and $Al_2O_3$ fibres. SiC whisker-reinforced ZTA has been extensively investigated by Claussen and coworkers [147–149].

Two of the difficulties associated with the reinforcement of ZTA by SiC whisker are uniform mixing and densification. The SiC whiskers will tend to be oxidized during pressureless sintering at high temperatures (e.g. 1600° C) [147]. Thus fabrication currently involves hot pressing and HIPing, with pressures ranging from 10 to 60 MPa, and temperatures from 1500 to 1800° C. In order to understand and control the interaction between SiC whiskers and the ZTA matrix it is important to study the structure and chemistry of the interfaces, which can be done using SEM and TEM. As reported by Claussen [149], ZTA reinforced by SiC whisker shows superior mechanical and thermal properties, for example, a toughness of 8 to 12 MPa $m^{0.5}$, and a strength of 700 to 1200 MPa, compared with 4 MPa $m^{0.5}$ and 500 MPa, respectively, for monolithic alumina. The authors concluded that the presence of the SiC whiskers in ZTA could result in a larger transformation zone as a consequence of the stress transfer by the whiskers, therefore generating a higher toughness, compared with a whisker-free ZTA. Multiple toughening mechanisms by zirconia (transformation toughening) and whiskers (crack deflection and pull-out) were proposed [148].

## 6. Conclusions

The toughening mechanisms and the microstructure–property relationship in ZTA have been reviewed. ZTAs with various structures have been shown to exhibit different toughening/strengthening mechanisms and mechanical properties. These composites can be fabricated by controlling powder preparation and densification processes. The mechanical properties at room temperature have been evaluated and understood. An optimum combination of the fracture strength and toughness can be made by controlling

(i) the relative amount of metastable tetragonal and monoclinic zirconia in the alumina matrix and therefore the relative amount of stress-induced transformation toughening and microcracking;

(ii) the particle size and stabilization of the zirconia additions; and

(iii) the degree of the agglomeration of the zirconia additions.

Selection of a specific structured material will be dependent on the particular application. Tougher composites are achieved in structures I and IV and stronger composites are achieved in structures II and III, respectively.

The future development of ZTAs will involve their reinforcement, property measurements and use at elevated temperature. A popular strategy for high-temperature property enhancement is SiC whisker reinforcement.

## Acknowledgement

The authors thank Dr J. G. P. Binner, Department of Ceramics, University of Leeds, for reading the manuscript of this paper.

## References

1. H. P. CAHOON and C. J. CRISTENSEN, *J. Amer. Ceram. Soc.* **39** (1956) 337.
2. N. CLAUSSEN, *ibid.* **59** (1976) 49.
3. N. CLAUSSEN and J. JAHN, *Ber. Dtsch. Keram. Ges.* **55** (1978) 487.
4. R. C. GARIVE, R. H. J. HANNINK and R. T. PASCOE, *Nature (London)* **258** (1975) 703.
5. F. F. LANGE, *J. Mater. Sci.* **17** (1982) 225.
6. N. CLAUSSEN, J. STEEB and R. F. PABST, *Amer. Ceram. Soc. Bull.* **55** (1977) 559.
7. "Phase Diagrams for Ceramists", No 4377-4388 (The American Ceramics Society, Columbus, Ohio, 1975).
8. R. M. McMEEKING and A. G. EVANS, *J. Amer. Ceram. Soc.* **65** (1982) 242.
9. A. G. EVANS and R. M. CANNON, *Acta Metall.* **34** (1986) 761.
10. N. CLAUSSEN and M. RUHLE in "Advances in Ceramics", Vol. 3, "Science and Technology of Zirconia I", edited by A. H. Heuer and W. L. Hobbs (The American Ceramics Society, Columbus, Ohio, 1981) p. 137.
11. A. G. EVANS (ed.) "Fracture in Ceramic Materials" (Noyes, New Jersey, 1984) p. 16.
12. J. C. LAMBROPOULOS, *J. Amer. Ceram. Soc.* **69** (1986) 218.
13. M. RUHLE, B. KRAUS, A. STRECKER and D. WAIDELICH, in "Advances in Ceramics", Vol. 12, "Science and Technology of Zirconia II", edited by N. Claussen, M. Ruhle and A. H. Heuer (The American Ceramics Society, Columbus, Ohio, 1984) p. 256.
14. A. G. EVANS, D. B. MARSHELL and N. H. BURLINGAME, in "Advances in Ceramics", Vol. 3, "Science and Technology of Zirconia I", edited by A. H. Heuer and L. W. Hobbs, (The American Ceramics Society, Columbus, Ohio, 1981) p. 202.
15. A. G. EVANS, in "Advances in Ceramics", Vol. 12, "Science and Technology of Zirconia II", edited by N. Claussen, M. Ruhle and A. H. Heuer (The American Ceramics Society, Columbus, Ohio, 1984) p. 193.
16. D. B. MARSHELL, A. G. EVANS and M. DRORY, in "Fracture Mechanics of Ceramics", Vol. 6, edited by R. C. Bradt, A. G. Evans, D. P. H. Hasselman and F. F. Lange (Plenum, New York, London, 1983) p. 289.
17. H. RUH and A. G. EVANS, *J. Amer. Ceram. Soc.* **66** (1983) 328.
18. A. G. EVANS and A. H. HEUER, *ibid.* **63** (1980) 241.
19. S. J. BURNS and J. R. MICHENER, in "Fracture Mechanics of Ceramics", Vol. 6, edited by R. C. Bradt, A. G. Evans, D. P. H. Hasselman and F. F. Lange (Plenum, New York, London,1983) p. 275.
20. L. A. ANDERSSON and T. K. GUPTA, in "Advances of Ceramics", Vol. 3, "Science and Technology of Zirconia", edited by A. H. Heuer and L. W. Hobbs (The American Ceramics Society, Columbus, Ohio, 1981) p. 184.
21. W. POMPE and W. KREHER, in "Advances in Ceramics", Vol. 12, "Science and Technology of Zirconia II", edited by N. Claussen, M. Ruhle and A. H. Heuer (The American Ceramics Society, Columbus, Ohio, 1984) p. 283.

22. A. G. EVANS, N. BURLINGAME, D. DRORY and W. M. KRIVEN, *Acta Metall.* **29** (1981) 447.
23. D. BROEK, "Elementary Engineering Fracture Mechanics", 3rd Edn (Martinus Nijhoff, Boston, Massachusetts, 1982).
24. L. R. F. ROSE and M. V. SWAIN, *J. Amer. Ceram. Soc.* **69** (1986) 203.
25. D. R. CLARKE and F. ADAR, *ibid.* **65** (1982) 284.
26. R. W. RICE, S. W. FREIMAN and P. F. BECHER, *ibid.* **64** (1981) 345.
27. R. W. RICE and S. W. FREIMAN, *ibid.* **64** (1981) 350.
28. F. F. LANGE, in "Fracture Mechanics of Ceramics", Vol. 6, edited by R. C. Bradt, A. G. Evans, D. P. H. Hasselman and F. F. Lange (Plenum, New York, London, 1983) p. 255.
29. R. C. GARVIE and M. V. SWAIN, *J. Mater. Sci.* **20** (1985) 1193.
30. R. C. GARVIE, *ibid.* **20** (1985) 3479.
31. A. G. EVANS and Y. FU, in "Fracture in Ceramics Materials", edited by A. G. Evans (Noyes, New Jersey, 1984) p. 560.
32. A. G. EVANS and K. T. FABER, *J. Amer. Ceram. Soc.* **64** (1981) 394.
33. K. T. FABER, in "Advances in Ceramics", Vol. 12, "Science and Technology of Zirconia II", edited by N. Claussen, M. Ruhle and A. H. Heuer (The American Ceramics Society, Columbus, Ohio, 1984) p. 293.
34. A. G. EVANS and Y. FU, *Acta Metall.* **33** (1985) 1525.
35. A. G. EVANS and K. T. FABER, *J. Amer. Ceram. Soc.* **67** (1984) 255.
36. L. R. F. ROSE, *ibid.* **69** (1986) 212.
37. Y. M. ITO and R. B. NELSON, in "Fracture Mechanics of Ceramics", Vol. 5, edited by R. C. Bradt, A. G. Evans, D. P. H. Hasselman and F. F. Lange (Plenum, New York, London, 1983) 479.
38. F. E. BURESCH, in "Advances in Ceramics", Vol. 12, "Science and Technology of Zirconia II", edited by N. Claussen, M. Ruhle and A. H. Heuer (The American Ceramics Society, Columbus, Ohio, 1984) p. 306.
39. D. J. GREEN, in "Fracture Mechanics of Ceramics", Vol. 5, edited by R. C. Bradt, A. G. Evans, D. P. H. Hasselman and F. F. Lange (Plenum, New York, London, 1983) p. 457.
40. A. J. GESING and R. C. BRADT, *ibid.*, p. 569.
41. A. G. EVANS and K. T. FABER, in "Fracture in Ceramics Materials", edited by A. G. Evans (Noyes, New Jersey, 1984) p. 109.
42. J. WANG and R. STEVENS, in "Proceedings of the British Ceramic Society", Vol. 39, edited by R. Freer, S. Newsam and G. Syers (British Ceramics Society, Stoke-on-Trent, 1987).
43. A. H. HEUER, F. F. LANGE, M. V. SWAIN and A. G. EVANS, *J. Amer. Ceram. Soc.* **69** (1986) i.
44. D. B. MARSHALL, *ibid.* **69** (1986) 173.
45. M. RUHLE, N. CLAUSSEN and A. H. HEUER, *ibid.* **69** (1986) 195.
46. S. HORI, M. YOSHIMURA and S. SOMIYA, *ibid.* **69** (1986) 169.
47. K. T. FABER and A. G. EVANS, *Acta Metall.* **31** (1983) 565.
48. T. W. COYLE and R. M. CANNON, *Amer. Ceram. Soc. Bull.* **60** (1981) 377.
49. R. RICE, *Ceram. Engng Sci. Proc.* **6** (1985) 589.
50. D. B. MARSHALL and R. JAMES, *J. Amer. Ceram. Soc.* **69** (1986) 215.
51. N. CLAUSSEN and D. P. H. HASSELMAN, in "Thermal Stresses in Severe Environment", edited by D. P. H. Hasselman and A. Heller (Plenum, New York, 1980) p. 381.
52. D. J. GREEN, F. F. LANGE and M. R. JAMES, in "Advances in Ceramics", Vol. 12, "Science and Technology of Zirconia II", edited by N. Claussen, R. Ruhle and A. H. Heuer (The American Ceramics Society, Columbus, Ohio, 1984) p. 240.
53. F. F. LANGE, *J. Amer. Ceram. Soc.* **63** (1980) 38.
54. D. J. GREEN and B. R. MALONEY, *ibid.* **69** (1986) 223.
55. N. CLAUSSEN, *Z. Werkstofft.* **31** (1982) 113.
56. D. J. GREEN, F. F. LANGE and M. R. JAMES, *J. Amer. Ceram. Soc.* **66** (1983) 623.
57. A. G. EVANS, *Philos. Mag.* **26** (1972) 1327.
58. J. WANG, PhD Thesis, Department of Ceramics, University of Leeds (1986).
59. N. CLAUSSEN, *J. Amer. Ceram. Soc.* **61** (1978) 85.
60. N. CLAUSSEN, R. L. COX and J. S. WALLACE, *ibid.* **65** (1982) C-190.
61. D. J. GREEN, *ibid.* **65** (1982) 610.
62. F. F. LANGE, in "Fracture Mechanics of Ceramics", Vol. 1, edited by R. C. Bradt, D. P. H. Hasselman and F. F. Lange (Plenum, New York, 1978) p. 3.
63. T. NOMA and A. SAMAOKA, *J. Mater. Sci. Lett.* **3** (1983) 533.
64. G. D. BOWLING, K. T. FABER and R. G. HOAGLAND, *J. Amer. Ceram. Soc.* **70** (1987) 849.
65. P. F. BECHER, *ibid.* **64** (1982) 37.
66. A. G. EVANS and W. BLUMENTHAL, in "Fracture Mechanics of Ceramics", Vol. 6, edited by R. C. Bradt, A. G. Evans, D. P. H. Hasselman and F. F. Lange (Plenum, New York, London, 1984) p. 423.
67. F. F. LANGE, R. I. DAVIS and D. R. CLARKE, *J. Mater. Sci.* **15** (1980) 601.
68. D. GREVE, N. CLAUSSEN, D. P. H. HASSELMAN and G. E. YOUNGBLOOD, *Amer. Ceram. Soc. Bull.* **56** (1977) 514.
69. L. BENTSEN, G. E. YOUNGBLOOD and N. CLAUSSEN, *Amer. Ceram. Soc. Bull.* **58** (1979) 342.
70. D. P. H. HASSELMAN, R. SYED and T. Y. TIEN, *J. Mater. Sci.* **20** (1985) 2549.
71. D. L. PORTER and A. H. HEUER, *J. Amer. Ceram. Soc.* **60** (1977) 183.
72. D. L. PORTER, A. G. EVANS and A. H. HEUER, *Acta Metall.* **27** (1979) 1649.
73. P. F. BECHER, *Acta Metall.* **34** (1986) 1885.
74. F. F. LANGE, *ICM*, **3**, Vol. 3 (Cambridge, 1979) 45.
75. A. H. HEUER, N. CLAUSSEN and W. M. KRIVEN, *J. Amer. Ceram. Soc.* **65** (1982) 642.
76. I. W. CHEN and Y. H. CHIAO, *Acta Metall.* **33** (1985) 1847.
77. I. W. CHEN, Y. H. CHIAO and K. T. SUZAKI, *ibid.* **33** (1985) 1847.
78. A. A. GRIFFITH, *Philos. Trans. R. Soc. London* **A221** (1921) 163.
79. M. RUHLE, A. G. EVANS, R. M. McMEEKING, P. G. CHARALAMBIDES and J. W. HUTCHINSE, *Acta Metall.* **35** (1987) 2701.
80. P. F. BECHER, *J. Amer. Ceram. Soc.* **66** (1983) 485.
81. LI-SHING LI, H. OLAPINSKI and R. F. PABST, in "Science of Ceramics 10", edited by H. Hausner (Deutsche Keramische Gesellschaft, 1980) p. 569.
82. R. F. PABST, I. BOGNAR and N. CLAUSSEN, *ibid.* p. 603.
83. G. ORANGE, G. FANTOZZI, R. TRABELSI, P. HOMERIN, F. THEVENOT, A. LERICHE and F. CAMBIER in "Science of Ceramics 14", edited by D. Taylor, R. Davidge, R. Freer, and D. T. Livery (Institute of Ceramics, Stoke-on-Trent, Staffs, 1988) p. 721.
84. K. TSUKUMA, K. UEDA and M. SHIMADA, *J. Amer. Ceram. Soc.* **68** (1985) C-4.
85. K. TSUKUMA, K. UEDA, K. MATSUSHITA and M. SHIMADA, *ibid.* **68** (1985) C-56.
86. K. TSUKUMA and M. SHIMADA, *J. Mater. Sci. Lett.* **4** (1985) C-857.
87. P. A. EVANS, PhD thesis, Department of Ceramics, University of Leeds (1984).
88. R. STEVENS and P. A. EVANS, *Br. Ceram. Trans. J.* **83** (1984) 28.
89. J. WANG and R. STEVENS, *J. Mater. Sci.* **23** (1988) 804.
90. I. NETTLESHIP and R. STEVENS, *J. Int. High Tech. Ceram.* **3** (1987) 1.
91. I. A. AKSAY, F. F. LANGE and B. I. DAVIS,

*J. Amer. Ceram. Soc.* **66** (1983) C-190.
92. E. A. PUGAR and P. E. D. MORGAN, *ibid.* **69** (1986) C-120.
93. Y. HIDEYUKI, A. OSAKA, *J. Mater. Lett.* **4** (1986) 426.
94. H. YOSHIMATSU, H. KAWASASI and A. OSAKA, *J. Mater. Sci.* **23** (1983) 332.
95. Y. MURASE, E. KATO and K. DAIMON, *J. Amer. Ceram. Soc.* **69** (1986) 83.
96. J. C. DEBSIKDAR,*J. Mater. Sci.* **22** (1987) 2237.
97. D. W. SPROSON and G. L. MESSING, *J. Amer. Ceram. Soc.* **67** (1984) C-92.
98. B. FEGLEY Jr, P. WHITE and H. K. BOWEN, *ibid.* **68** (1985) C-60.
99. S. HORI, M. YOSHIMURA and S. SOMIYA, in "Advances in Ceramics", Vol. 12, "Science and Technology of Zirconia II", edited by N. Claussen, M. Ruhle and A. H. Heuer (The American Ceramics Society, Columbus, Ohio, 1984) p. 794.
100. M. KAGAWA, M. KIKUCHI, Y. SYONO and T. NAGAE, *J. Amer. Ceram. Soc.* **66** (1983) 751.
101. N. CLAUSSEN, G. LINDEMAN and G. PETZOW, in "Ceramics Powders", edited by Vincenzini (Elsevier, Essex, 1983).
102. J. ECHIGOYA, Y. TAKABAYASHI, H. SUTO and M. ISHIGAME, *J. Mater. Sci. Lett.* **5** (1986) 150.
103. J. ECHIGOYA, Y. TAKABAYASHI, K. SASAKI, S. HAYASHI and H. SUTO, *Trans. Jpn. Inst. Metals* **27** (1986) 102.
104. J. ECHIGOYA and H. SUTO, *J. Mater. Sci. Lett.* **5** (1986) 949.
105. M. YOSHIMURA, S. KIKUGAWA and S. SOMIYA, *Yogyo-Kyokai-Shi* **91** (1983) 182.
106. I. W. CHEN and Y. H. CHIAO, in "Advances in Ceramics", Vol. 12, "Science and Technology of Zirconia II", edited by N. Claussen, M. Ruhle and A. H. Heuer (The American Ceramics Society, Columbus, Ohio, 1984) p. 23.
107. G. DEPORTU and C. FIORI, presented at the Third International Conference on Science and Technology of Zirconia, III, Tokyo, Japan, September (1986), "Advances in Ceramics", in press.
108. J. REQUENA, R. MORENO and J. S. MOYA, Proceedings of the British Ceramics Society, Vol. 38, "Novel Ceramic Fabrication Processes and Applications", edited by R. W. Davidge (British Ceramics Society, Stoke-on-Trent, 1986) p. 101.
109. J. D. KATZ, R. D. BLAKE and J. J. PETROVIC, in "Ceramics Abstract", 89th Annual Meeting of the American Ceramics Society 1987 (American Ceramics Society, Columbus, Ohio, 1987).
110. C. H. HSUCH, A. G. EVANS and R. L. COBLE, *Acta. Metall.* **30** (1982) 1296.
111. F. J. ESPER, K. H. FRIESE and H. GEIER, in "Advances in Ceramics", Vol. 12, "Science and Technology of Zirconia II", edited by N. Claussen, M. Ruhle and A. H. Heuer (The American Ceramics Society, Columbus, Ohio, 1984) p. 528.
112. F. F. LANGE, *J. Amer. Ceram. Soc.* **66** (1983) 396.
113. S. BAIK, A. BLEIER and F. P. BECHER, *Mat. Res. Soc. Symp. Proc.* **73** (1986) 791.
114. F. WAKAI and H. KATO, *Adv. Ceram. Mater.* **3** (1988) 71.
115. F. F. LANGE and M. METCALF, *J. Amer. Ceram. Soc.* **66** (1983) 398.
116. F. F. LANGE and B. I. DAVIS, *ibid.* **66** (1983) 407.
117. F. F. LANGE and M. M. HIRLINGER, *ibid.* **67** (1984) 164.
118. F. F. LANGE and B. I. DAVIS, in "Advances in Ceramics", Vol. 12, "Science and Technology of Zirconia II", edited by N. Claussen, M. Ruhle and A. H. Heuer (The American Ceramics Society, Columbus, Ohio, 1984) p. 699.
119. S. P. KRAUS-LANTERI, T. E. MITCHELL and A. H. HEUER, *J. Amer. Ceram. Soc.* **69** (1986) 256.
120. B. W. KIBBEL and A. H. HEUER, in "Advances in Ceramics", Vol. 12, "Science and Technology of Zirconia II", edited by N. Claussen, M. Ruhle and A. H. Heuer (The American Ceramics Society, Columbus, Ohio, 1984) p. 415.
121. *Idem, J. Amer. Ceram. Soc.* **69** (1986) 231.
122. S. HORI and R. KURITA, presented at the Third International Conference on Science and Technology of Zirconia III, Tokyo, Japan, September (1986), "Advances in Ceramics", in press.
123. F. F. LANGE and M. M. HIRLINGER, *ibid.* **70** (1987) 827.
124. S. C. H. KOH, K. A. AIR and R. McPHERSON, in "Advances in Ceramics", Vol. 24, Science and Technology of Zirconia III. Edited by S. Somiya, N. Yamamoto and H. Hanagida (American Ceramics Society, Westerville, Ohio, 1988) p. 293.
125. F. F. LANGE, B. I. DAVIS and E. WRIGHT, *J. Amer. Ceram. Soc.* **69** (1986) 66.
126. R. L. COBLE, J. E. BURKE in "Processes in Ceramics Science", Vol. 3, edited by J. E. Burke (Macmillan, New York, 1963) p. 197.
127. T. KOSMAC, J. S. WALLACE and N. CLAUSSEN, *J. Amer. Ceram. Soc.* **65** (1984) 242.
128. M. I. OSENDI and J. S. MOYA, *J. Mater. Sci. Lett.* **7** (1988) 15.
129. B. YANG and R. STEVENS, unpublished work (1989).
130. R. RUH and H. J. GARRETT, *J. Amer. Ceram. Soc.* **50** (1967) 257.
131. S. HORI, M. YOSHIMURA, S. SOMIYA and H. KAJI, *J. Mater. Sci. Lett.* **3** (1984) 242.
132. M. V. SWAIN, *J. Amer. Ceram. Soc.* **68** (1985) C-97.
133. *Idem, Acta Metall.* **33** (1985) 2083.
134. M. V. SWAIN and L. R. F. ROSE, *J. Amer. Ceram. Soc.* **69** (1986) 511.
135. N. CLAUSSEN, *Mater. Sci. Engng* **71** (1985) 23.
136. *Idem.* in "Advances in Ceramics", Vol. 12, "Science and Technology of Zirconia II", edited by N. Claussen, M. Ruhle and A. H. Heuer (American Ceramics Society, Columbus, Ohio, 1984) p. 325.
137. T. SATO and M. SHIMADA, *J. Amer. Ceram. Soc.* **67** (1984) C-212.
138. F. F. LANGE, G. L. DUNLOP and B. I. DAVIS, *ibid.* **69** (1986) 237.
139. C. BAUDIN and J. S. MOYA, in "Science of Ceramics 14" edited by D. Taylor, R. Davidge, R. Freer and D. T. Livery (Institute of Ceramics, Stoke-on-Trent, Staffs, 1988) p. 831.
140. M. ISHITSUKA, T. SATO, T. EDDO and M. SHIMADA, *J. Amer. Ceram. Soc.* **70** (1987) C-342.
141. J. M. RINCON, T. R. DINGER, G. THOMAS, J. S. MOYA and M. I. OSENDI, *Acta Metall.* **35** (1987) 1175.
142. T. SATO, H. FUJISHIRO, T. ENDO and M. SHIMADA, *J. Mater. Sci.* **22** (1987) 882.
143. T. K. BROG, J. S. WALLACE and T. Y. TIEN, in "Fracture Mechanics of Ceramics", Vol. 8, edited by R. C. Bradt, A. G. Evans, D. P. H. Hasselman and F. F. Lange (Plenum, New York, London, 1984) p. 143.
144. T. Y. TIEN, T. K. BROG and A. K. LI, *Int. J. High Tech. Ceram.* **2** (1986) 207.
145. "Phase Diagrams for Ceramists", no. 4444 (American Ceramics Society, Columbus, Ohio, 1975).
146. L. J. SCHIOLER and J. J. STIGLICH Jr, *Amer. Ceram. Soc. Bull.* **65** (1986) 289.
147. N. CLAUSSEN, K. L. WEISSKOPF and M. RUHLE, *J. Amer. Ceram. Soc.* **69** (1986) 288.
148. N. CLAUSSEN and G. PETZOW, *Mater. Sci. Res.* **20** (1986) 649.
149. *Idem, J. de Physique* **47** (1986) c1.

*Received 27 June*
*and accepted 20 December 1988*